

An explainable predictive maintenance strategy for multi-fault diagnosis of rotating machines using multi-sensor data fusion

Shreyas Gawde ^{a,c}, Shruti Patil ^b, Satish Kumar ^{b,*}, Pooja Kamat ^a, Ketan Kotecha ^b

^a Symbiosis Institute of Technology (SIT), Symbiosis International (Deemed) University, Pune, India

^b Symbiosis Centre for Applied Artificial Intelligence (SCAAI), Symbiosis Institute of Technology, Symbiosis International (Deemed University), Pune, India

^c Goa University, Taleigao Plateau, Goa, 403206, India



ARTICLE INFO

Keywords:

Industry 4.0
Explainable artificial intelligence
Predictive maintenance
Multi-fault diagnosis
Multi-sensor data fusion
Industrial rotating machines

ABSTRACT

Industry 4.0 denotes smart manufacturing, where rotating machines predominantly serve as the fundamental components in production sectors. The primary duty of maintenance engineers is to upkeep these vital machines, aiming to reduce unexpected halts and extend their operational lifespan. The most recent development in smart maintenance is Predictive Maintenance (PdM). Due to the diversity of machinery and the diverse behaviour of each machine in different fault conditions, the most challenging task in predictive maintenance is to detect the fault, diagnose the type of fault, and explain why a particular fault is predicted. This study proposes an effective Explainable Predictive Maintenance strategy considering (1) test setup building, (2) low-cost Fast Fourier Transform (FFT) raw data using multiple sensors, (3) multi-sensor data fusion, (4) comparing various multi-class classification algorithms, (5) analysis of cases concerning multi-sensor versus single sensor and multi-location versus single location, and (6) explainable predictive maintenance. Quantitative results from this study reveal a remarkable multi-fault detection accuracy and multiple fault type classification, with the highest accuracy of 100%. Furthermore, multi-sensor data fusion significantly outperforms single-sensor approaches, demonstrating an enhancement in fault prediction accuracy of all models. Using Explainable Artificial Intelligence methods contributes to the interpretability of fault diagnoses, making it a critical advancement in Intelligent Manufacturing and Predictive Maintenance in Industry 4.0. The study's novelty is using Explainable Artificial Intelligence (Local Interpretable Model Agnostic Explanation (LIME) and Random Forest) for multi-fault classification of rotating machines using multi-sensor data fusion.

1. Introduction

Historically, industries relied on domain experts to diagnose faults in the machinery. These procedures, however, are time-consuming and prone to human error. As a result, intelligent approaches must be devised, particularly for rotating machines, which are crucial in plant operations, especially in production Industries. Predicting the status of machine components is critical to avoid catastrophic failures. Predictive maintenance is a technique currently developing and consists of the generation, processing, interpretation, or analysis of data indicating the current state of critical components in the industrial process. Several researchers are constantly upgrading this technique, which is still developing due to the diversity of machinery in industries and the diversity in the behaviour of each machinery for different fault conditions. Various factors need to be considered for Predictive maintenance. The data collected is an essential factor to be considered for the high accuracy of results in Predictive maintenance. Data Acquisition (DAQ)

has been challenging due to various factors such as availability of the test setup, simulation of faults, specifications of data acquisition device, sensors to be used, and the expense associated with this. These factors are influenced mainly by the component to be studied and the measurement techniques employed. Also, due to online datasets that mainly focus on single-component faults, extensive literature is available on single-component faults such as bearing faults. However, practically, one fault may give rise to another, simultaneously causing multiple faults in the machinery [1]. Hence, some researchers have started focusing on multiple fault diagnosis employing their test setup and data collection. Many articles also focus on "Vibration analysis" as it is a proven method for early fault diagnosis [2]. Other methods, such as "Thermography", "Motor current signature analysis", "Magnetic Chip Detectors", "Ultrasound", "Acoustic Analysis", etc., are also widely used [3–5]. The detailed bibliometric literature survey and systematic literature survey on this topic are done by authors in [6,7]. This raw data collected by researchers in the time domain is challenging to

* Corresponding author.

E-mail addresses: shreyasgwd@gmail.com, shreyasgwd@unigoa.ac.in (S. Gawde), shruti.patil@sitpune.edu.in (S. Patil), satishkumar.vc@gmail.com (S. Kumar), pooja.kamat@sitpune.edu.in (P. Kamat), director@sitpune.edu.in (K. Kotecha).

Table 1
Literature review concerning multiple aspects of predictive maintenance.

References	Multi fault diagnosis	Sensor Selection	Frequency domain raw data	Multiple Sensor use	Data Acquisition	Feature Extraction	Feature processing	Multi-fault classification algorithms	Explainable AI	Challenges	Future Scope	Overview
[1]	●	-	●	●	-	●	●	●	-	●	●	Multi-fault diagnosis using SVM and frequency domain
[8]	●	-	●		-	●	●	●	-	●	●	Multi-fault diagnosis using SVM
[1-4]	●	-	-	-	-	-	-	●	-	●	●	Multi-fault diagnosis using Deep CNN and SVM
[1-5]	●	-	-	●	●	●	●	●	-	●	●	Multi-sensor DAQ system for fault detection
[1-6]	-	●	-	-	●	●	●	●	-	●	●	DAQ system for CM of rotating machines

validate at the data acquisition stage due to the complexity of the signal. One cannot explain the validity of the data collected, which is the most essential and primary component in Predictive maintenance. Hence, recently, some literature has started focusing on direct frequency-domain raw data collection, specifically the Fast Fourier Transform (FFT) raw data [1,8], for data-driven fault diagnosis. FFT data gives signature frequency peaks that can be used to validate the data (while being) collected for a particular type of fault simulation, which is impossible in time-domain raw data. FFT provides a clear separation between each type of defect and a quantifiable variation in the distribution of accumulated damage over time. This article attempts to consider this FFT raw data for Predictive maintenance. Finally, various Artificial Intelligence (AI) models are used to classify faults [2]. The AI models include Support Vector Machine [9], Random Forest [10], Decision Tree [11], Artificial Neural Network [12], Convolutional Neural Network [2], Recurrent Neural Network [13], etc., that has given a considerable amount of accuracy. However, these models, being the black box models, are inefficient in explaining their decisions. The maintenance of critical machines is highly cost-consuming; hence, there needs to be a clear explanation of the decisions made by the AI Models to make them trustworthy. Explainable AI (XAI) is another emerging aspect of Artificial Intelligence considered in this article.

Before moving ahead, it is crucial to look at the work currently being done in the field: “Explainable Multiple Fault Diagnosis in Rotating Machines using FFT Data”. The status of the work is detailed in the bibliometric review and systematic literature review by the authors in [6,7]. Apart from this, Table 1 describes the status of the current work of some closely related literature [1,8,14-16] concerning various aspects such as:

- Are the articles about rotating machine multi-fault diagnosis?
- Have the authors talked about sensor selection?
- Are there multiple sensors used for analysis?
- Has frequency domain raw data (FFT Data) been used for the analysis?
- Is there a detailed procedure on how to do data acquisition?
- Is there a discussion on extracting features and further implementing feature processing?
- Have the articles given explanations for the results?
- What are the various Artificial Intelligence approaches for multi-fault classification?
- What are the key barriers and future outlook for this field?

Table 2 analyses recent articles using frequency domain raw data analysis for explainable multi-fault diagnosis in rotating machines.

It is seen that most literature collects time-domain raw data, which is later processed to convert into frequency-domain data. Also, very few articles explore explainable artificial intelligence-based multi-fault diagnosis in rotating machines. Based on Tables 1 and 2, the following are the observed research gap and the future direction for the upcoming research:

- Most literature does not mention the validity of the data (while being) collected from the simulated fault due to the use of complex time domain signals for analysis. FFT raw data can reveal more information about the data being collected while validating the simulated fault.
- Researchers have used their test setups for experimentation using FFT raw data; however, very little literature focuses on the systematic building of test setups. Addressing the systematic building of test setups will allow future researchers to build setups, allowing multiple aspects to be explored in this domain.
- Most of the literature employing FFT raw data has not emphasized factors to consider while making sensor selections or how to make your data acquisition system. There is a need to address multiple aspects of the data acquisition system, such as sensors, mounting of sensors, data collection, data mapping, data fusion, etc.
- Most researchers have used a single type of analysis, such as vibration or sound analysis, for fault diagnosis using FFT data. Each technique has its benefit in detecting a particular type of fault. There is a need to fuse multiple techniques using multiple sensors for multiple fault diagnosis.
- Explainable AI (XAI) is a concept yet to be considered and an emerging area that can significantly affect overall Predictive maintenance, increasing the trust in decisions made by the black-box AI models.

Table 2 focuses on articles purely in the domain of Predictive Maintenance of rotating machines. XAI is a novel field currently being investigated and it can be seen that very few articles are focusing on implementing Explainable Artificial Intelligence (XAI) in Predictive Maintenance. Let us analyse the literature available on XAI implemented in various domains through Table 3.

To address the issues mentioned in the above literature survey, this paper presents a systematic implementation of predictive maintenance for explainable multiple fault diagnosis such as no-fault, overhung rotor unbalance, two-plane rotor unbalance, offset misalignment, component looseness, and bearing faults in rotating machines using raw FFT Data. The study has also covered all the aspects related to data acquisition, feature extraction, multi-sensor data fusion, and various multi-class

Table 2

Literature review concerning frequency domain raw data analysis for explainable multi-fault diagnosis in rotating machines.

Refer- ence	Type of fault	Sensors	Type of data collected	Data-driven algorithms used	Explainable artificial intelligence	Limitations
[17]	“Multi-fault” (wind turbine energy systems under various faulty scenarios.)	“Multi-sensor”	“Time domain data collected. Data from the time domain was processed to create frequency domain data.”	Fast Fourier Transform (FFT) + Principal Component Analysis (PCA)	Not Used	The approach does not give an explanation of the results.
[18]	“Multi-fault” (Healthy, Misalignment, Bent shaft, rubbing shaft, Bearing Looseness, and Shaft with breathing crack)	“Multi-sensor”	”	Linear Classifier + Principal Component Analysis	Not Used	The approach does not give an explanation of the results.
[19]	“Single component fault” (Bearing fault)	“Multi-sensor”	”	Extreme learning machine (ELM)	Not Used	Multiple types of faults are not considered. The approach does not explain the results.
[20]	“Multi-fault” (Bearing fault, Unbalance, Broken bar)	“Single-sensor”	”	Artificial Neural Network	Not Used	The approach does not give an explanation of the results. Multiple types of sensors are not used.
[21]	“Multi-fault” (Solenoid operated valve fault cases)	“Multi-sensor”	”	Support Vector Machine, Decision Tree, K-Nearest Neighbours (KNN), Random Forest, Deep Neural Network	Not Used	The approach does not give an explanation of the results.
[22]	“Single component fault” (Bearing fault)	“Single sensor”	“FFT was extracted from raw vibration data.”	Support Vector Machine (SVM)	Not Used	Multiple types of faults are not considered. The approach does not give an explanation of the results. Multiple types of sensors are not used.
[23]	“Single component fault” (Bearing fault)	–	“Time domain data collected. Data from the time domain was processed to create frequency domain data.”	Artificial Neural Network (ANN)	Not Used	Multiple types of faults are not considered. The approach does not give an explanation of the results.
[24]	“Single component fault” (Bearing fault)	“Single sensor”	”	Support Vector Machine	Not Used	Multiple types of faults are not considered. The approach does not give an explanation of the results. Multiple types of sensors are not used.
[25]	“Single component fault” (Gear fault)	“Multi-sensor”	”	Convolutional Neural Network (CNN)	Not Used	Multiple types of faults are not considered. The approach does not give an explanation of the results.
[26]	“Single component fault” (Bearing fault)	“Single sensor”	”	Convolutional Neural Network	Not Used	Multiple types of faults are not considered. The approach does not give an explanation of the results. Multiple types of sensors are not used.
[27]	“Single component fault” (Gear fault)	“Single sensor”	”	Support Vector Machine	Not Used	Multiple types of faults are not considered. The approach does not give an explanation of the results. Multiple types of sensors are not used.
[28]	“Single component fault” (Centrifugal pump faults)	“Multi-sensor”	“FFT Data extracted from sensors.”	Support Vector Machine with Gaussian Radial Basis Function	Not Used	Multiple types of faults are not considered. The approach does not give an explanation of the results. Multiple types of sensors are not used.
[29]	The article focuses on the presence or absence of fault.	“Multi-sensor”	“Time domain data collected. Data from the time domain was processed to create frequency domain data.”	Linear Regression, Support Vector Machine, Optimized Artificial Neural Network, and XG Boost.	Not Used	The proposed method does not classify or identify the fault in the machinery. The approach does not give an explanation of the results.
[30]	The article focuses on Real-time machine data.	“Multi-sensor”	“Time domain data collected. Data from the time domain was processed to create frequency domain data.”	Not Used	Not Used	The proposed method does not classify or identify faults in the machinery. The approach does not give an explanation of the results.

(continued on next page)

Table 2 (continued).

Reference	Type of fault	Sensors	Type of data collected	Data-driven algorithms used	Explainable artificial intelligence	Limitations
[32]	“Single component fault” (Bearing Faults)	Multiple Vibration sensors	“Time domain data collected.”	Neural Network (NN)	Not Used	Multiple types of sensors are not used. The approach does not give an explanation of the prediction. Multiple types of faults are not considered.
[33]	“Multi-fault” (Gear faults, bearing faults, and induction motor faults)	“Single sensor”	“Time domain data collected.”	Naïve Bayes, K-Nearest Neighbours, Recurrent Neural Network, and Support Vector Machine	Not Used	Multiple types of sensors are not used. The approach does not give an explanation of the results.
[34]	“Single component fault” (Bearing Faults)	“Single sensor”	“Time domain data collected. Data from the time domain was processed to create frequency domain data.”	Convolutional Neural Network	Decision Tree	Multiple types of sensors are not used. Analysis was done on the Online dataset only. Validation on test setup not implemented. Multiple types of faults are not considered.
[35]	“Single component fault” (Bearing Faults)	“Single sensor”	“Time domain data collected. Data from the time domain was processed to create frequency domain data.”	K-Nearest Neighbours	Additive Shapley explanation	Multiple types of sensors are not used. Multiple types of faults are not considered.
[36]	“Multi-fault” (Normal case, Bearing faults, Gearbox faults, Unbalance, misalignment, Looseness)	“Single sensor”	“Time domain data collected. Data from the time domain was processed to create frequency domain data.”	Clustering Based Local Outlier Factor, Local Outlier Factor, Isolation Forest, Lightweight online detector of anomalies, Histogram-based Outlier Detection, k-nearest Neighbours, Fast - Angle-based Outlier Detector, Outlier Detection with Minimum Covariance Determinant, One-Class Support Vector Machine, Feature Bagging and Ensemble	Shapley additive explanations, Local depth-based feature importance for the isolation forest	Multiple types of sensors are not used.
[37]	“Single component fault” (Bearing Faults)	“Single sensor”	–	–	Not Used	The approach does not explain the prediction. Multiple types of faults are not considered.
[38]	“Single component fault” (Bearing Faults)	“Single sensor”	“Time domain data collected.”	Convolutional Neural Network- Visual Geometry Group-16 (VGG16)	Local Interpretable Model-Agnostic Explanations	Multiple types of sensors are not used. Analysis was done on the Online dataset only. Validation on test setup not implemented. Multiple types of faults are not considered.

classification algorithms, which are mostly not considered in detail in the literature available. Most available literature has focused separately on time-domain raw [30] vibration data for fault diagnosis and prognosis. To our knowledge, much work has not been done to gather direct frequency domain raw data (FFT Data) for fault diagnosis and subsequent prediction and explanation using Explainable AI. In this case, the raw FFT data denotes the direct output of the vibration sensor as the raw FFT data instead of collecting the data in the time domain and then processing the data to the frequency domain. This article has used and analysed frequency domain raw data to validate the data collected. To illustrate the effectiveness of the proposed DAQ system, a case study is presented in which the multiple faults are classified using various multi-class classification algorithms, giving high accuracy of results. The results are also explained using Local Interpretable Model Agnostic Explanation (LIME) and Random Forest (RF). The innovation of this study work is using frequency domain raw data (FFT data) using multi-sensor data fusion for multi-fault classification and explaining the classification using Local Interpretable Model Agnostic Explanation (LIME) and Random Forest (RF).

1.1. Contribution of work

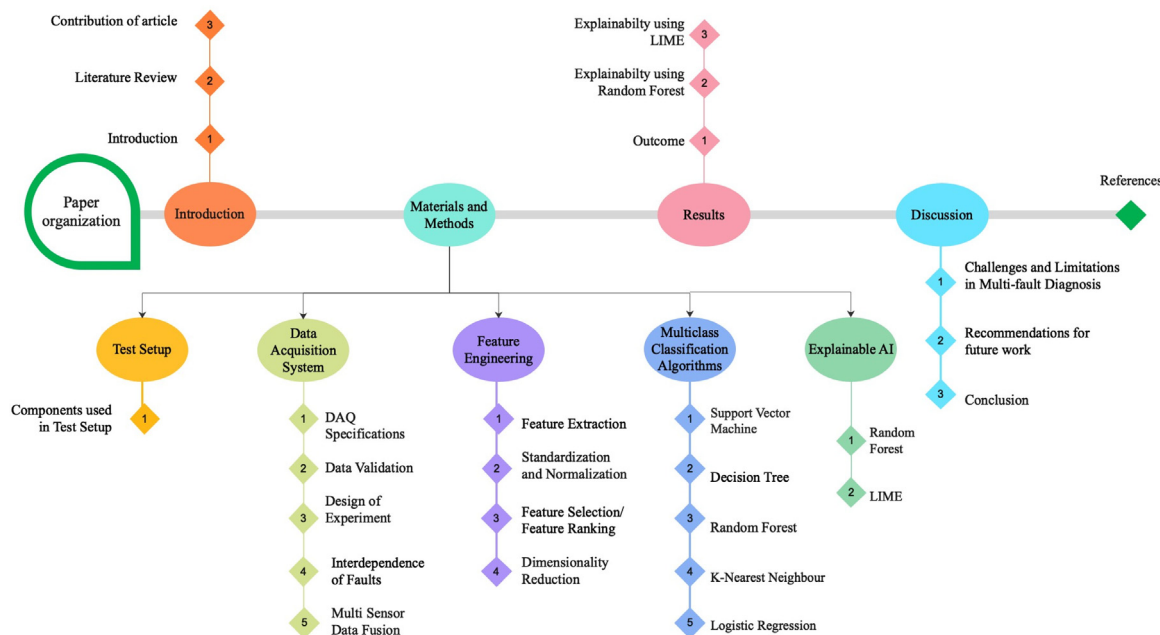
In traditional predictive maintenance, machine learning models predict when equipment will likely fail, helping organizations schedule maintenance proactively. However, these models often operate as “black boxes”, making it challenging to understand why a particular prediction was made. Explainability becomes crucial because it provides insights into the factors contributing to equipment failure predictions. This transparency allows maintenance teams to make informed decisions, understand the root causes of potential failures, and prioritize maintenance tasks effectively. Explainable predictive maintenance is essential because it combines the benefits of predictive maintenance with transparency and interpretability. The novelty of the research lies in the use of “Explainable Artificial Intelligence” while considering the aspects mentioned ahead:

- Frequency Domain Analysis: Frequency domain analysis methods can unfold more information based on frequency features which are difficult to detect in the time domain raw data. This paper

Table 3

Literature review concerning explainable artificial intelligence in various domains. [39–48].

Reference	Domain	Shapley Additive Explanations (SHAP)	Local Interpretable Model-Agnostic Explanations (LIME)	Tree-based explanations	Light Gradient Boosting Machine (LightGBM)	Layer-wise Relevance Propagation (LRP)	Counterfactual Explanations
[39]	XAI in Healthcare	●	●				
[40]	XAI in Job cycle time prediction			●			
[41]	XAI in the Water Pumping Industry			●			
[42]	XAI in Agriculture	●	●		●		
[43]	XAI in Autonomous Vehicles		●				
[44]	XAI in Online Beauty Health	●					
[45]	XAI in Jet taggers					●	
[46]	XAI in Industry 4.0					●	
[47]	XAI in Intrusion Prevention	●	●				
[48]	XAI in Data Envelopment Analysis						●

**Fig. 1.** Paper organization.

focuses on frequency domain raw (FFT) data and its detailed analysis. The FFT raw data collected is also validated using real-time industrial VibeXpert II.

- **Multiple Sensors:** The traditional methods include vibration, temperature, and acoustic signals for fault detection in rotating machines. The effectiveness of using a combination of different techniques using multiple sensors for fault analysis is substantiated in this paper. For this purpose, the accelerometer, temperature, and current sensor data are fused.
- **Multiple Faults:** It is seen that the literature available considers a single type of fault analysis. However, in practical cases, it is seen that one fault gives rise to another fault. This paper

considers multiple faults and the interdependence of faults in rotating machines.

- **Data Acquisition:** This article also discusses in detail the steps for fault detection in rotating machines using FFT data, right from sensor selection, the building of test setup, bearing selection, availability of online data, data acquisition, multiple sensor data fusion, and feature extraction to implementation of AI algorithms.
- **Explainable Predictive Maintenance:** The article discusses using Explainable AI (XAI) in predictive maintenance using LIME and Random Forest (RF).

The paper's organization is shown in Fig. 1.

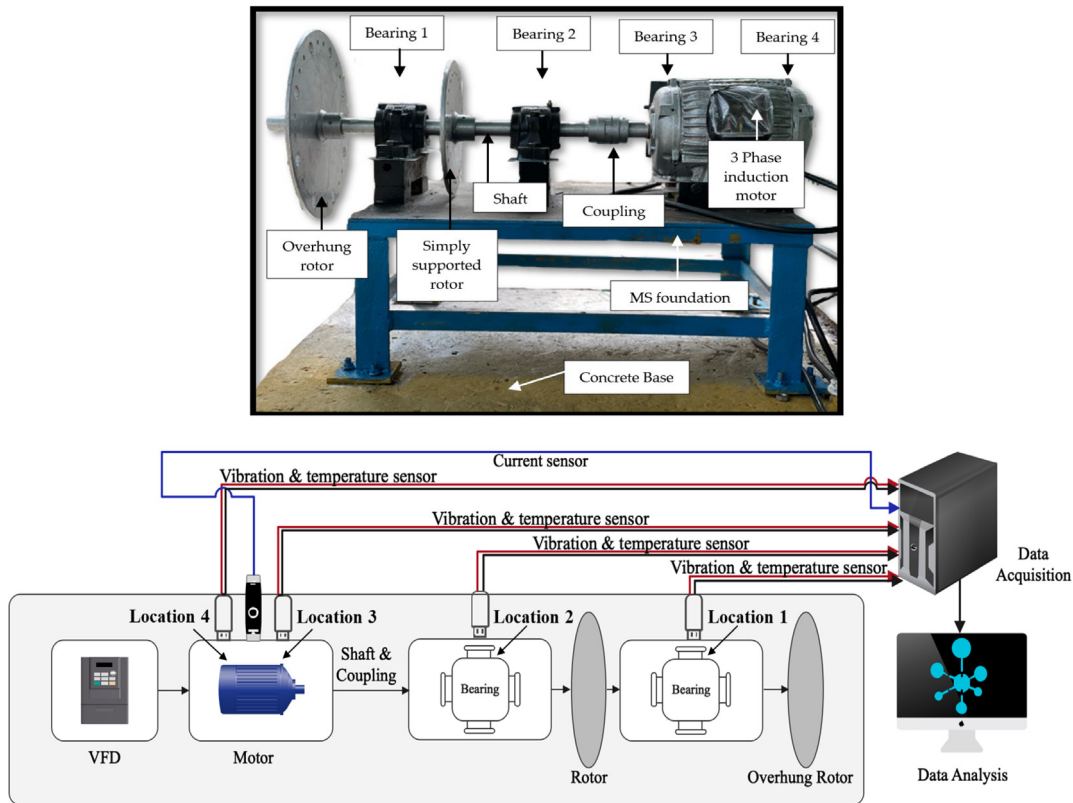


Fig. 2. Test setup for experimentation.

2. Materials and methods

This section explores all the methods and materials needed for multi-fault diagnosis in rotating machines, beginning with a test setup followed by a data acquisition system, feature engineering, multi-class classification algorithms and explainable AI.

2.1. Test setup

The data can be collected in two ways: using an online dataset [49–51] and collecting the data from the test setup [52,53] using sensors. Various online platforms are available for online datasets related to bearing test rigs, “Case Western Reserve University” being the widely used dataset. The other platforms are the “FEMTO” Dataset, “Intelligent Maintenance Systems” (IMS) Dataset, “NASA Prognostic Centre of Excellence” dataset, “Mandeville” Dataset, “Paderborn University” Dataset, “IEEE Dataport”, “Machinery Failure Prevention Technology” (MFPT) Dataset, “SpectraQuest’s Machinery Fault Simulator (MFS) Alignment-Balance-Vibration (ABVT)”, etc.

Online datasets give monetary benefits while saving time in making and designing a test setup. However, it does not give data freedom, which may lead to incomplete diagnosis or misdiagnosis [54]. Also, online datasets are mostly related to single-component faults, mainly bearing-related faults; as a result, multi-fault diagnosis is impossible. Hence, it is preferred to build a test setup for data collection. Ready test rigs are available by SpectraQuest, Inc. or Tyrannus Innovative Engineering & Research Academy. The data should be ideally collected from industrial rotating machines, which is not possible due to industrial protocols and uncontrollable conditions on the site. Hence, it is ideal for making a test setup as per your requirements, which saves cost to an extent compared to buying the test rig. The key points to make a test setup for simulating multiple faults are discussed below.

2.1.1. Components in test setup

The proposed test bench (Fig. 2) consists of a 3 phase induction motor, Variable Frequency Drive (VFD), shaft with a diameter of 3 cm and total length of 95 cm, three-jaw spider coupling that connects the two shafts from the driver and the driven end, two Timken 22207KEJW33C3 double row spherical bearings, two deep groove ball bearings in induction motor and two rotors (simply supported rotor with diameter 25 cm and overhung rotor with diameter 35 cm). The setup is mounted on a Mild Steel (MS) foundation strongly supported on the concrete base. The test setup is designed to simulate bearing faults, unbalance, misalignment, and structural looseness. The following subsections discuss different components in brief.

Motor: The driver unit comprises three 3-phase, 2.2 kW, 3 hp, 4-pole induction motor. The maximum speed achievable is calculated using the formula given below in Eq. (1) [55]:

$$\text{Speed of motor} = \frac{120 * f}{p} \quad (1)$$

Where f is the “frequency” and p is the “number of poles”. Accordingly, the maximum motor speed in the test setup is 1500 rpm. The frequency control in the motor is carried out by 3HP Danfoss VLT Microdrive FC 51 with a multi-featured front panel. The motor base is made movable. Jack bolts can be used for horizontal misalignment, and standard shims for vertical misalignment. The base is also pinned for easy realignment. The motor used can be seen in Fig. 2.

Load: Load is the most relevant parameter in condition monitoring of rotating machines since vibration rates differ up to 10%–15% between normal and no-load operations. Also, the bearing size depends on the magnitude of the load to be applied. To achieve load in the test setup, an overhung rotor with a diameter of 350 mm and thickness of 7 mm and a simply-supported rotor with a diameter of 250 mm and thickness of 7 mm is mounted on a 950 mm long shaft with a 30 mm diameter. Weight of the overhung rotor (approx.) = mass $\times g$ = $5.4 \text{ kg} \times 9.81 \text{ m/s}^2 = 52.974 \text{ N}$. The weight of the simply-supported rotor (approx.) = $3.087 \text{ kg} \times 9.81 \text{ m/s}^2 = 30.283 \text{ N}$. The rotors are

Table 4

List of the defect frequencies of each bearing component for different rotational speeds.

22207KEJW33C3	Frequency Hz	Speeds		
		800 RPM	1000 RPM	1200 RPM
BPFO	6.4 * RPS (Revolution per Second)	85.33	106.66	128.00
BPFI	9.324 * RPS	124.316	155.403	186.48
BSF	2.88 * RPS	38.399	48.001	57.6
FTF	0.583 * RPS	7.773	9.717	11.66

equipped with 24 threaded holes each, 15 degrees apart, to induce unbalance in the test setup. Fig. 2 shows the two rotors used in the test setup.

Bearing: Bearing is the component that facilitates the relative motion between the static and movable parts of any rotating machinery. The factors considered while choosing the bearing in the test setup are load, speed, and shaft dimensions, especially concerning bore diameter. The bearings would also be employed to run until failure. Hence, the price factor was also considered. There are various manufacturers, such as SKF, FAG, TIMKEN, etc., that provide a wide variety of bearings. Based on the conditions mentioned above, TIMKEN 22207KEJW33C3, double row-spherical roller bearing, is used in the test setup (locations 1 & 2, Fig. 2). The bearing is fastened to the shaft using TIMKEN SNT 507-606 split plummer block, which is provided with the threaded opening to screw-mount the accelerometers for vibration monitoring. The induction motor employs two 6206-2Z deep groove ball bearings from SKF on the drive and non-drive end (locations 3 & 4, Fig. 2). It is mandatory to identify all the bearing locations to achieve complete machinery vibration data.

Rolling Element Bearing (REB) consists of an inner ring, outer ring, rolling element, cage, and seal. If any of these elements have a surface abnormality, a cluster of high-frequency vibrations is created each time the defect meets the race or element. These clusters of high-frequency vibration occur at a pace specified by the bearing design and the motor's Rotations Per Minute (RPM). These recurring frequency rates are referred to as bearing fault frequencies. There are four fault frequencies associated with REB as given in Eq. (2) to (5) [5]:

“Ball Pass Frequency Outer (BPFO) or Outer race defect”

$$= \frac{N}{2} fr \left\{ 1 - \frac{Rd}{Pd} \cos\alpha \right\} \quad (2)$$

“Ball Pass Frequency Inner (BPFI) or Inner race defect”

$$= \frac{N}{2} fr \left\{ 1 + \frac{Rd}{Pd} \cos\alpha \right\} \quad (3)$$

“Ball Spin Frequency (BSF) or Rolling element defect”

$$= \frac{Pd}{Rd} fr \left\{ 1 - \left(\frac{Pd}{Rd} \cos\alpha \right)^2 \right\} \quad (4)$$

“Fundamental Train Frequency (FTF) or Cage defect frequency”

$$= \frac{fr}{2} \left\{ 1 \pm \frac{Rd}{Pd} \cos\alpha \right\} \quad (5)$$

(+ sign if the outer race is rotating, - sign if the inner race is rotating); N= “No. of rolling elements”; fr= “Shaft rotational speed, Hz”; Rd= “Rolling element diameter”; Pd= “Pitch circle diameter”; α = “Contact angle”.

A list of the defect frequencies of each bearing component for different rotational speeds is presented in Table 4, in line with the geometric parameters of the TIMKEN bearing employed. These frequencies were obtained from the Timken website.

2.2. Data acquisition

Data collection is crucial in Condition Monitoring (CM) of rotating machines. The features of Data Acquisition (DAQs) systems and the cost they represent are significant impediments to deploying the DAQ system. The data acquisition process includes acquiring sensor data and processing the raw signal to extract essential features that may be utilized to assess the system's health. This latter approach is referred to as feature engineering in data science and is explored in the following sections.

2.2.1. Data acquisition specifications

Various options related to the Data AcQuisition (DAQ) system are discussed in detail in [7]. Following are the Components of the DAQ system used for bearing test rig.

Sensors: According to ISO 13373-1, accelerometers are used to quantify the vibration level in the rotating machinery. The vibration level depicts the health of the machinery. This test setup uses four industrial grade, screw lock-type, stainless steel, and triaxial vibration gauge VB-310 SCB. Before buying a vibration sensor, the key points to be considered concerning the multi-fault diagnosis of rotating machines are [7] frequency response (Hz), acceleration range (g), sensitivity, temperature, data acquisition system hardware/ interface, wired/wireless, sensor mounting and computing technique.

Besides the accelerometer, four temperature sensors, MAX6675, which can sense temperature from 00 C to 10240 C with a measurement resolution of 0.250 C, are also screw-mounted on bearings. Similarly, the test setup has a PZEM-004T current sensor with TTL serial interface, working voltage: 80 ~ 260VAC, rated power: 100A/22000 W, and measurement accuracy: 0.5%. The resolution for the current is 0.001 A, the voltage resolution is 0.1 V, and the active power resolution is 0.1 W. This sensor is wrapped around the electrical cable that supplies power to the motor. Temperature and current sensors are advantageous in early anomaly detection.

Mounting of Sensors: According to ISO 13373, It is ideal to have a sensor permanently mounted using a stud or screw mounting, and the cable must not be curved with a radius smaller than 50 mm (2.0 in.) and should be secured to reduce the stress at the cable end points. Other mounting techniques include direct adhesive cement, hand-held, and magnetic mounting. According to ISO 13373, the best location to mount the accelerometer and temperature sensors is at a right angle to the shaft on the surface free from oil and grease and closest to the source of vibration (e.g., bearings).

The test setup is structured horizontally. There are four bearings (location of interest) in the test setup. It is also important to note that the test setup is designed to simulate multiple faults at multiple locations. To achieve accurate data on machinery conditions, it is therefore critical to collect the data from each bearing location simultaneously. Hence, there are four accelerometers and four temperature sensors mounted, one on each bearing perpendicular to the surface of the bearing. The current sensor is mounted around the motor wiring. Because of the multiple sensors used, there is a need for a data acquisition system with multi-sensor data fusion, which is discussed in the upcoming sections.

Connecting the data acquisition system: Accelerometer VB-310 SCB has an integrated design, with a sensor and transducer in one mini package. The output signals are already industrial RS-485. The output contents include 3-axis velocity-acceleration RMS (Root Mean Square), 3-axis velocity-acceleration FFT, and 3-axis displacement-peak-peak. The VB-310 SCB collects time-domain data internally converted to FFT data, giving direct FFT raw data as the output. The sensor can be directly connected to 3rd party Programmable Logic Controller (PLC) and Distributed Control System (DCS) without requiring DAQ using open signal protocols (MODBUS Remote Terminal Unit (RTU)). For the sensor to be connected to a Personal Computer (PC), an RS485 to Universal Serial Bus (USB) converter is used. The accelerometer is set up to get FFT velocity data in the X, Y, or Z direction.

The PZEM 004T current sensor primarily measures AC voltage, current, active power, frequency, power factor, and active energy. The

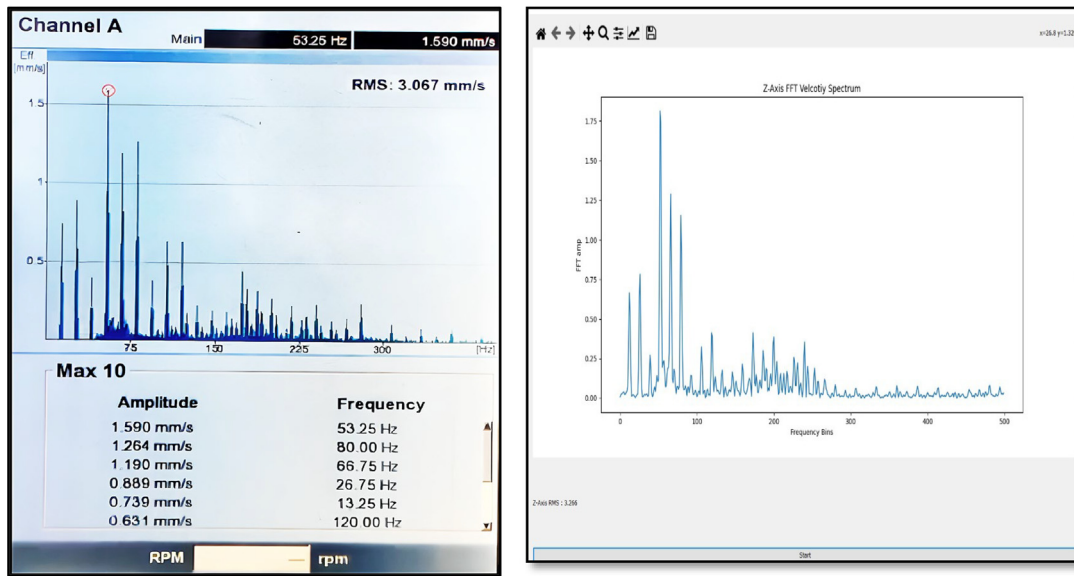


Fig. 3. FFT Spectrum on VibXpert II and data acquisition technique used, respectively.

PZEM 004T current sensor enables data transfer through an RS485 communication interface, ensuring compatibility with a PC for data acquisition. The MAX6675 thermocouple temperature sensor can be securely attached to the bearing housing. MAX6675 is connected to Arduino via SPI protocol. The Arduino UNO is configured as a Modbus slave using the “ModbusRTUslave” library and is directly linked to the PC without the need for any converter. In the setup, the VB310 SCB and PZEM 004T connect to the PC via a USB to RS485 converter, while the MAX6675 is linked to the PC through the Arduino UNO. The Modbus-RTU protocol is employed at the application layer for communication with all sensors. A Python application has been developed to interface with and gather data from the mentioned devices. The collected data is then stored in a CSV file, ready to be utilized by an AI algorithm for further analysis.

The challenging task in DAQ is implementing multi-sensor data fusion, which handles homogeneous and heterogeneous data as the data can be from a similar type of multiple sensors or multiple types of multiple sensors.

The cost of one accelerometer ranges from Rs. 15,000 to Rs. 25,000/-, MAX6675 thermocouple temperature sensor cost ranges from Rs. 300 to Rs. 500/-, PZEM 004T current sensor ranges from Rs. 1000/- to Rs. 1500/-, RS485 to USB module costs from Rs. 500/- to Rs. 1000/- . All these sensors can be directly connected to a computer system without requiring an expensive DAQ system using open signal protocols (MODBUS RTU), thus drastically reducing the cost of DAQ Setup.

2.2.2. Data validation

Data is validated using Pruftechnik's VibXpert II, a widely used portable device by condition monitoring experts for recording and analysing machine condition data quickly and reliably in the industrial environment. The VibXpert II has a frequency range from 0.5 Hz to 51.2 KHz with a sampling frequency rate of up to 131 KHz per channel. The FFT spectrum generated by VibXpert II was validated with the FFT spectrum generated from the data Acquired from the test setup while the data was being collected. The top 5 frequency peaks were validated on both the Data Acquisition devices, which were found accurate at the respective frequencies. The top 5 frequencies at which the peaks were recorded using the data acquisition technique discussed are 53 Hz, 66 Hz, 80 Hz, 26 Hz and 13 Hz, similar to the frequency peaks obtained on VibXpert II. Fig. 3 compares the FFT Spectrum on VibXpert II and the data acquisition technique. Thus, collecting frequency-domain raw data enables the researchers to validate the data being collected at the crucial data acquisition stage, which may not be possible if time-domain raw data is collected.

2.2.3. Design of experiment

The details of the test setup are given in Section 2.1. Different faults are artificially seeded at different locations in the test setup to perform fault analysis. The test setup is configured to operate at three different rotational speeds: 800 rpm, 1000 rpm, and 1200 rpm. A total of 27 different fault conditions/ machinery conditions (at multiple speeds) are considered in the test setup, which is broadly classified as (I) No fault, (II) Overhung rotor unbalance, (III) Two plane rotor unbalance, (IV) Offset misalignment (V) Component looseness and bearing defects such as (VI) Inner race defect, (VII) Outer race defect, (VIII) Rolling element defect, and (IX) Cage defect [6] for all the different test setup speed configurations.

The single-plane unbalance condition is seeded in the test setup by adding additional weight at location 1. The two-plane unbalance is seeded in the test setup by adding additional weight at location 1 and location 2, as shown in the test setup. The misalignment condition is seeded in the test setup by offsetting the motor location, thus changing the alignment near the coupling at location 3. Component looseness was seeded in the test setup by loosening the bearing housing at location 1. Bearing defects were induced in the bearing by drilling at the inner race, outer race, rolling elements, and cage at locations 1 and 2. The details of the different machinery conditions, data acquisition sequence, and the corresponding number of datasets generated are given in Table 5. A single dataset contains three-axis vibration sensor FFT data at each of 4 locations, one temperature sensor data at each of 4 locations, and one current sensor data as shown in Table 6.

Measurements were taken for the rotational speed of 26.6 Hz (800 rpm), 33.3 Hz (1000 rpm), and 40 Hz (1200 rpm). 150 sets of data (FFT) were taken for each machinery condition. Each FFT consists of 2000 data points. A total of 2000×150 (FFT) samples were collected for each of three directions (i.e., x, y, and z directions) at each speed by each accelerometer for each machinery condition ($2000 \times 150 \times 3 \times 3 \times 4 \times 9$ samples). Similarly, temperature data were also collected by four temperature sensors at each bearing location ($2000 \times 150 \times 4 \times 3 \times 9$ samples), and a single current sensor captured current data ($2000 \times 150 \times 1 \times 3 \times 9$ samples) at each speed for each machinery condition. Following are details of the total data collected from multiple sensors.

- Sampling rate: 8000 Hz
- FFT frequency resolution: 1 Hz
- No. of samples/dataset in the frequency domain (a): 2000 samples
- No. of datasets (b): 150 datasets per speed

Table 5

Details of data acquisition sequence.

Fault category	Machinery condition	Speeds			Total sets
		800 rpm	1000 rpm	1200 rpm	
No fault	No fault	150 datasets	150 datasets	150 datasets	450
Unbalance	Overhung rotor unbalance	150 datasets	150 datasets	150 datasets	
	Two-plane rotor unbalance	150 datasets	150 datasets	150 datasets	1350
Misalignment	Offset misalignment	150 datasets	150 datasets	150 datasets	1350
	Inner race defect	150 datasets	150 datasets	150 datasets	
Bearing defect	Outer race defect	150 datasets	150 datasets	150 datasets	1800
	Rolling element defect	150 datasets	150 datasets	150 datasets	
	Cage defect	150 datasets	150 datasets	150 datasets	
Looseness	Component looseness	150 datasets	150 datasets	150 datasets	900

Table 6Details of data collected in one dataset from [Table 5](#).

Location 1		Location 2		Location 3		Location 4	
Vib Sens 1	Temp	Vib. Sens 2	Temp	Vib. Sens 3	Temp	Vib. Sens 4	Temp
X-axis FFT	sens. 1	X-axis FFT	sens. 2	X-axis FFT	sens. 3	X-axis FFT	sens. 4
(2000 data points)	Current						
Vib Sens 1	Vib Sens 2	Vib Sens 3	Vib Sens 4	Vib Sens 1	Vib Sens 2	Vib Sens 3	Vib Sens 4
Y axis FFT	Y axis FFT	Y axis FFT	Y axis FFT	(2000 data points)	(2000 data points)	(2000 data points)	(2000 data points)
(2000 data points)	(2000 data points)	(2000 data points)	(2000 data points)	Vib Sens 1	Vib Sens 2	Vib Sens 3	Vib Sens 4
Vib Sens 1	Vib Sens 2	Vib Sens 3	Vib Sens 4	Z axis FFT	Z axis FFT	Z axis FFT	Z axis FFT
Z axis FFT	Z axis FFT	Z axis FFT	Z axis FFT	(2000 data points)	(2000 data points)	(2000 data points)	(2000 data points)
(2000 data points)	(2000 data points)	(2000 data points)	(2000 data points)	Vib Sens 1	Vib Sens 2	Vib Sens 3	Vib Sens 4

- No. of measurements using four tri-axial accelerometers (c): 4 sensors*3 axis= 12
- Number of measurements using four temperature and one current sensor (d): 5
- Number of fault conditions (e): 9
- Total data collected per fault at a single speed (f)= $a*b*(c+d)$: 51,00,000
- Total data collected for all faults at a single speed (g)= $f*e$: 4,59,00,000
- Total data collected (h)= $g*(3 \text{ speeds})$: 13,77,00,000

The FFT spectrum of the raw data for 'no fault' and 'fault' is plotted in [Fig. 4a](#), respectively. The frequency response of the accelerometer is from 1 Hz to 2000 Hz, which means that velocity amplitude was recorded at every hertz. It can be seen that the frequency activity is within 500 Hz for the current system under test. Frequencies above 500 Hz give near-zero amplitude. Hence, instead of considering data at higher frequencies (where there is not much vibration activity), a better resolution may be chosen to capture intricate frequencies, as seen in [Fig. 4b](#). This gives more details about characteristic fault frequencies. For further analysis, 1 to 500 Hz data is considered instead of 1 to 2000 Hz.

2.2.4. Interdependence of fault

During data collection, it was observed that the different machinery/fault conditions are not independent. One fault may give rise to another [3], as seen in [Fig. 4b](#), a plot of unbalance condition. Unbalance is depicted by high amplitude at 1x shaft rotational speed. Many harmonics of the shaft rotational speed in the frequency spectrum indicate looseness. Harmonic peaks of the same frequency (1x, 2x, 3x, etc.) might arise in the spectra depending on the evolution of the looseness. Both the signs are seen in [Fig. 4b](#). However, it is seen that these harmonics of shaft rotational speeds have an acceptable amplitude. The continued running of the machinery may lead to an increase in the amplitude of these multiple peaks, where there is a need to consider the presence of two faults at a time/ interdependence of faults.

2.2.5. Multi-sensor data fusion

Data-level, feature-level, and decision-level fusion [56] are the three fusion technology types. Each method of fusing has advantages and disadvantages. The fusion method typically depends on the application area and the types of sensors used. Data from comparable sensors are merged directly in the data-level fusion approach. The fused data is classified using the AI classification algorithm following feature extraction. In feature-level fusion, each sensor is utilized to capture the signal. Following that, feature extraction is used to generate a feature vector. All features are merged to determine the best feature subset, fed into a classifier or decision-level fusion. Feature-level fusion is used for data fusion in this article. At the decision-level fusion stage, feature calculation and fault classification methods are applied sequentially to single-source data acquired from each sensor. The decision vectors are then fused using decision-level fusion methods.

Feature-level fusion is shown in [Fig. 5](#) [57]. Firstly, data is acquired from multiple sensors, as discussed above, with each sensor capturing unique insights into the machine's condition. Subsequently, feature extraction is performed independently for each sensor, generating sets of features that describe the machine's state. The core of feature-level fusion involves amalgamating the extracted features from all sensors into a single feature vector. To achieve this, careful data mapping from multiple sensors has to be implemented at the data acquisition stage. In our case, FFT data from 4 sensors at three axis, temperature data from 4 sensors and current data from 1 sensor (Total= $((4*3) + 4 + 1) = 17$) were mapped as one set ([Table 6](#)). Multiple features (discussed ahead) were extracted from this set and mapped as a single feature vector, achieving feature-level fusion. Following the fusion, various machine learning methods can be applied to detect and diagnose faults within the machine, as discussed further.

2.3. Feature engineering

The process of choosing, transforming, extracting, integrating, and manipulating raw data to provide the required variables for improved analysis or predictive modelling is known as feature engineering. The following steps were taken on the collected data to achieve authentic results.

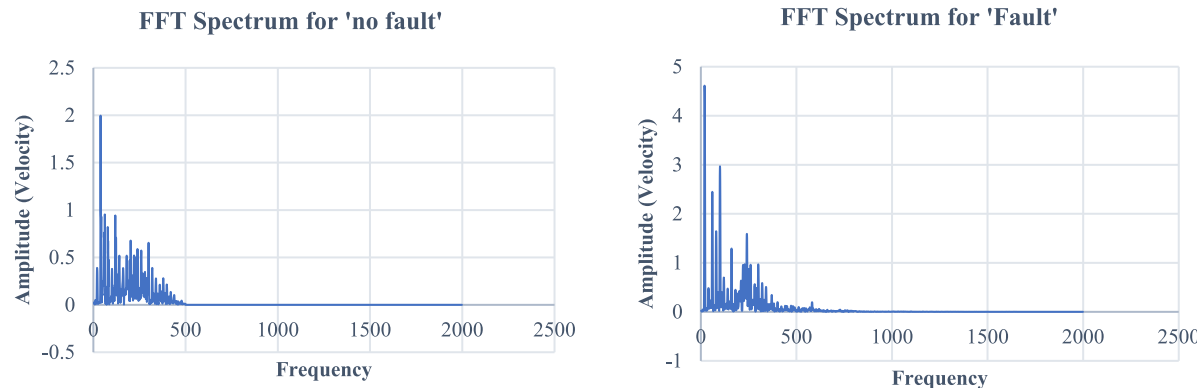


Fig. 4a. FFT spectrum for 'no fault' & 'fault data' for frequency range 1–2000 Hz at 1200 rpm, respectively.

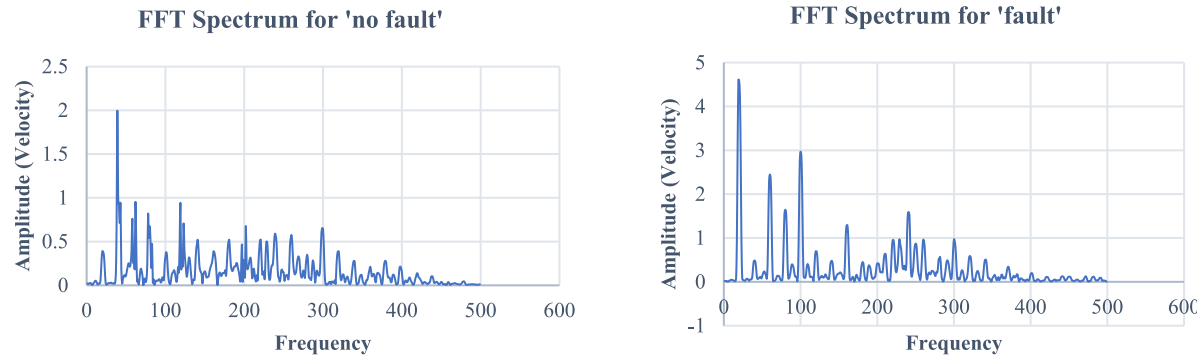


Fig. 4b. FFT spectrum for 'no fault' & 'fault data' for frequency range 1–500 Hz at 1200 rpm.

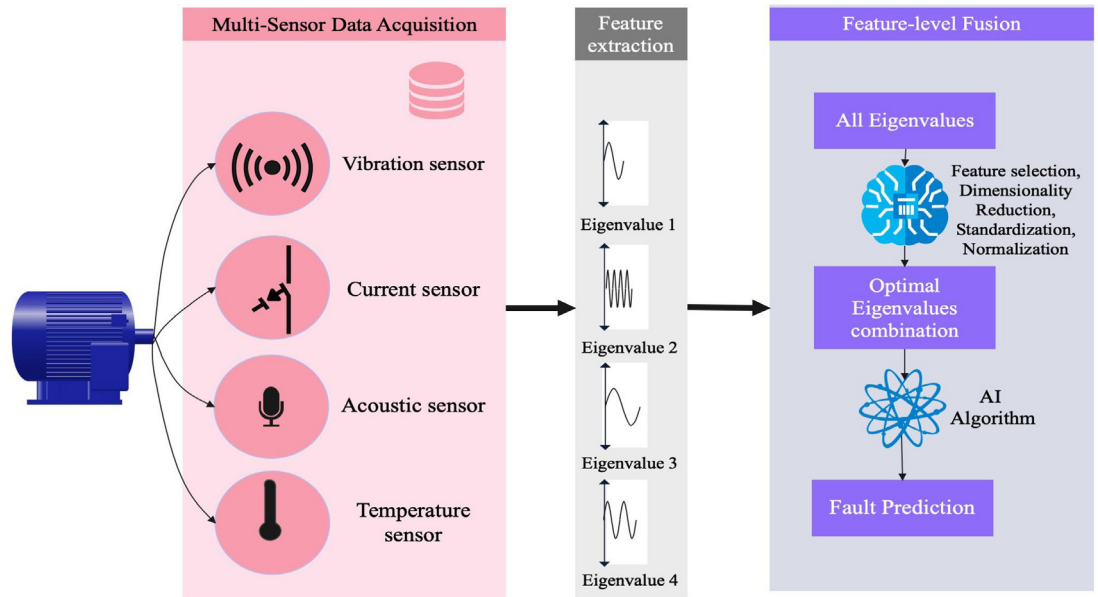


Fig. 5. Feature-level fusion.

2.3.1. Feature extraction

The data collected have a high dimensionality, as seen in Section 2.2.3. As a result, if these data are utilized for training the classifier directly, the classification results may be unsatisfactory. As a result, appropriate statistical features that hold fault information and are sensitive to fault severity variations must be chosen. Statistical features [58,59], as shown in Table 7, are extracted from FFT data. All these features are fused and arranged for further analysis. Table 7 lists the standard definitions of all of these features. Here, N is the Nyquist

frequency, and the amplitude of the frequency spectrum at a frequency "i" is represented by " X_i ".

11 statistical features \times 3 axis = 33 statistical features are calculated from each dataset, that is, from 2000 samples (FFT) in the x, y and z-axis. A total of 150 rows of feature sets are collected in three directions for each speed at each location. In other words, 34 columns (i.e., a total of 33 statistical feature columns + 1 column for data label) \times 150 rows feature set is available for each fault at each speed at each location. For nine different faults/ machinery conditions (i.e., no-fault, overhung

Table 7

Feature extraction from FFT data.

Feature	Significance	Formula
Mean μ	“Average of vibration signal throughout a measured signal”	$\mu = \frac{1}{N} \sum_{i=0}^N X_i$
Variance μ_2	“The second central moment of data distribution” represents how much a collection of data is spread out from its Mean.	$\mu_2 = \frac{1}{N} \sum_{i=0}^N (X_i - \mu)^2$
Standard deviation σ	“The square root of the variance” is used to quantify the degree of dispersion of a set of data values.	$\sigma = \sqrt{\mu_2}$
Skewness (S)	“The measure of the asymmetrical behaviour of vibration signal through its probability distribution of real-valued data about its mean”. Faults impact the symmetry of distribution and increase skewness.	$\frac{\frac{1}{N} \sum_{i=0}^N (X_i - \mu)^3}{\sigma^3}$
Kurtosis (K)	“The fourth standardized moment of the data distribution and is a measure of the tailedness of probability distribution of real-valued data about its mean”.	$\frac{\frac{1}{N} \sum_{i=0}^N (X_i - \mu)^4}{\sigma^4}$
Root Mean Square	“Signifies the energy content in the signal”. RMS value increases as the fault develops.	$RMS = \sqrt{\frac{1}{N} \sum_{i=0}^N X_i ^2}$
Root Sum of Squares (RSS)	“The method by which the standard uncertainties of many contributors are integrated to yield our total combined uncertainty”	$RSS = \sqrt{\sum_{i=0}^N X_i ^2}$
Sum of Squares (SS)	“Divergence of data points from the mean value”. More SS result denotes more dataset variability, and a lower score denotes less significant departures from the Mean.	$SS = \sum_{i=0}^N X_i ^2$
Shape Factor w	“RMS divided by the absolute value’s mean” independent of the signal dimensions, relies on the signal shape.	$w = \frac{RMS}{\mu}$
Impulsion Index I	“The ratio of the peak value to the average of the absolute value of the vibration signal”.	$I = \frac{\max X_i }{\mu}$
Crest Factor P	“The ratio of the vibration signal’s peak amplitude to its RMS amplitude”. Faults often manifest themselves in changes in the peakiness of the signal before they manifest in energy represented by RMS.	$P = \frac{\max X_i }{RMS}$
Temperature	An increase in temperature depicts the development of faults in the machinery.	–
Current	An increase in current depicts the development of faults in the machinery.	–

$FC_{1x(f(1,1)800)}$...	$FC_{1x(f(11,1)800)}$	$FC_{1y(f(1,1)800)}$...	$FC_{1y(f(11,1)800)}$	$FC_{1z(f(1,1)800)}$...	$FC_{1z(f(11,1)800)}$
\vdots		\vdots	\vdots		\vdots	\vdots		\vdots
$FC_{1x(f(1,150)800)}$...	$FC_{1x(f(11,150)800)}$	$FC_{1y(f(1,150)800)}$...	$FC_{1y(f(11,150)800)}$	$FC_{1z(f(1,150)800)}$...	$FC_{1z(f(11,150)800)}$
$FC_{1x(f(1,1)1000)}$...	$FC_{1x(f(11,1)1000)}$	$FC_{1y(f(1,1)1000)}$...	$FC_{1y(f(11,1)1000)}$	$FC_{1z(f(1,1)1000)}$...	$FC_{1z(f(11,1)1000)}$
\vdots		\vdots	\vdots		\vdots	\vdots		\vdots
$FC_{1x(f(1,150)1000)}$...	$FC_{1x(f(11,150)1000)}$	$FC_{1y(f(1,150)1000)}$...	$FC_{1y(f(11,150)1000)}$	$FC_{1z(f(1,150)1000)}$...	$FC_{1z(f(11,150)1000)}$
$FC_{1x(f(1,1)1200)}$...	$FC_{1x(f(11,1)1200)}$	$FC_{1y(f(1,1)1200)}$...	$FC_{1y(f(11,1)1200)}$	$FC_{1z(f(1,1)1200)}$...	$FC_{1z(f(11,1)1200)}$
\vdots		\vdots	\vdots		\vdots	\vdots		\vdots
$FC_{1x(f(1,150)1200)}$...	$FC_{1x(f(11,150)1200)}$	$FC_{1y(f(1,150)1200)}$...	$FC_{1y(f(11,150)1200)}$	$FC_{1z(f(1,150)1200)}$...	$FC_{1z(f(11,150)1200)}$

Box I.

rotor unbalance, two-plane unbalance, offset misalignment, component looseness, inner race fault, outer race fault, cage fault, rolling element fault), a total of $34 \text{ columns} \times 9 \text{ rows} \times 150 \text{ rows}$ of the feature set is available at each speed at a single location. A total of 3 different speeds are considered. As a result, $34 \text{ columns} \times 150 \text{ rows} \times 9 \text{ rows} \times 3 \text{ rows}$ is the final feature set for all faults, in all axis, at all speeds, for all features from a single location. The feature matrix (34 columns and 450 rows) of a single fault/ machinery condition from a single location is shown in the Box I. Note that the feature matrix explained above is only for the vibration data. The additional feature column of temperature and current data is taken as it is from the data collected. Also, note that this data was simultaneously collected from 4 different sensor locations (multiple locations) in the test setup. This total feature set is divided and used for training, optimizing the parameters, and final testing in the simulation. In the matrix shown in Box I, FC_1 denotes the Fault Condition 1 followed by the x, y, or z axis. $f(1,1)800$ depicts feature no.

1 of the first row (or of 1st set of FFT) at 800 rpm. $f(1,150)1200$ depicts feature no. 1 of 150th row (or of 150th set of FFT) at 1200 rpm. With this nomenclature, $FC_{1z(f(11,150)1200)}$ represents Feature no. 11 of the 150th row (or of the 150th set of FFT) of Fault Condition 1 in the z-axis at 1200 rpm. There is also a final column for fault labels not depicted in the matrix. The data analysis was carried out for various combinations to evaluate the necessity of single sensor v/s multiple sensors, single location v/s multiple locations, and the combination of the two.

Case 1: Fault detection using a single-sensor at a single-location: A single vibration sensor detects the fault at single locations. The related sensor is placed at one location irrespective of the fault locations for different cases. For example, an unbalance was induced in the overhung rotor. However, the sensor was mounted at bearing location 2 (refer to Fig. 2). Similarly, all the data was collected by the sensor at location 2 for all the fault cases. A total of 33 features (without current and temperature) were extracted from the X, Y, and Z axis from a single

sensor for each fault at three different speeds. Hence, the feature matrix comprises $[(33*1)+1]$ columns and 450 rows for each fault condition.

Case 2: Fault detection using a single-sensor at multiple locations: A single vibration sensor detects the fault at multiple locations. The related sensor is placed at each bearing location. For example, the misalignment was induced at the coupling, and the sensor was mounted at bearing locations 1, 2, 3, and 4 (refer to Fig. 2). A total of 33 features (without current and temperature) were extracted from X, Y, and Z axis from each sensor for each fault at three different speeds. Hence, the feature matrix comprises $[(33*4)+1]$ columns and 450 rows for each fault condition.

Case 3: Fault detection using multiple sensors at a single-location: In this case, multiple sensors like vibration, temperature, and current were used to detect the fault at a single location. The related sensors were placed nearest to the fault location. For example, unbalance was induced in the overhung rotor; hence, the sensors were mounted at bearing location 1 (refer to Fig. 2). A total of 33 features (extracted from the X, Y, and Z axis) + 1 current + 1 temperature from each sensor location for each fault at three different speeds. Hence, the feature matrix comprises $[((33+1)*1)+1+1]$ columns and 450 rows for each fault condition.

Case 4: Fault detection using multiple sensors at multiple locations: In this case, multiple sensors like vibration, temperature, and current were used to detect the fault at multiple locations. The related sensor is placed at each bearing location. For example, the misalignment was induced at the coupling, and the sensors were mounted at bearing locations 1, 2, 3, and 4 (refer to Fig. 2). A total of 33 features (extracted from X, Y, and Z axis) + 1 current + 1 temperature from each sensor location for each fault at three different speeds. Hence, the feature matrix comprises $[((33+1)*4)+1+1]$ columns and 450 rows for each fault condition.

Out of all features, the ones that did not show variation in data for different fault classes were discarded using feature selection methods discussed in subsequent sub-sections. Systematic analysis of all four cases is done using machine learning techniques, and the result is analysed in the following section 5.

2.3.2. Standardization and Normalization

Feature scaling is the most essential step in AI [60]; otherwise, algorithms that calculate the distance between the features are skewed towards numerically bigger values. Among the most commonly used feature scaling methods are normalization and standardization.

Normalization or min–max scaling is necessary only when features have diverse ranges. For example, the temperature range may be from 25 to 100; however, the current calculated is from 0 to 5. The vibration sensor range is different again. In this case, normalization is necessary. The range is scaled to [0, 1] or sometimes [-1, 1]. The formula for normalization is as given in Eq. (6).

$$X_{\text{new}} = (X - X_{\text{min}})/(X_{\text{max}} - X_{\text{min}}) \quad (6)$$

Transforming data into a standardized format so users may process and evaluate it is known as data standardization or Z-score normalization. By deducting from the Mean and dividing by the Standard Deviation (Std), features are transformed to become standardized. The Z-score is a common name for this. The formula for standardization is as given in Eq. (7).

$$X_{\text{new}} = (X - \text{mean})/\text{Std} \quad (7)$$

We apply standardization to ensure a zero mean and a unit standard deviation.

2.3.3. Feature selection/feature ranking

The feature selection technique aims to remove redundant or unnecessary features and use only the relevant features that can be utilized to create effective models of the phenomenon under study [61]. Feature selection's primary objectives are to enhance a predictive model's performance, reduce overfitting and lower the model's computational expense. There are two categories of feature selection techniques: supervised and unsupervised. Wrapper techniques (forward, backward, and stepwise selection), filter methods (ANOVA, Pearson correlation, variance thresholding), and embedding methods (Lasso, Ridge, Decision Tree) are again three subcategories of supervised techniques.

Techniques such as Random Forest [61] and XGBoost Classifier were used for feature ranking for all 4 cases. We are presenting results for the Multi-sensor Single Location case as it achieved a high accuracy discussed in subsequent sections. Here, 9 features were finally selected for the Multi Sensor Single Location feature set. Fig. 6 plots important features in the Multi-sensor Single Location case using the Random Forest classifier.

2.3.4. Dimensionality reduction

Feature selection is merely choosing some features to include or exclude from a given feature set. However, the dimensionality reduction technique reduces the features in dimension. PCA (Principal Component Analysis) is a dimensionality reduction technique to identify and represent the most important patterns and structures in high-dimensional data. It aims to transform the original features into a new set of uncorrelated variables called Principal Components (PCs) [62]. These PCs are either the same number or fewer than the original features included in the dataset. The principal components are sorted based on their corresponding eigenvalues in descending order. The principal component with the highest eigenvalue captures the maximum variance in the data. The top-k principal components that explain most of the variance are chosen. These selected principal components form a new feature subspace with reduced dimensionality. PCA was employed in all 4 cases from Section 3.1. to see how the data gets classified using the principal components.

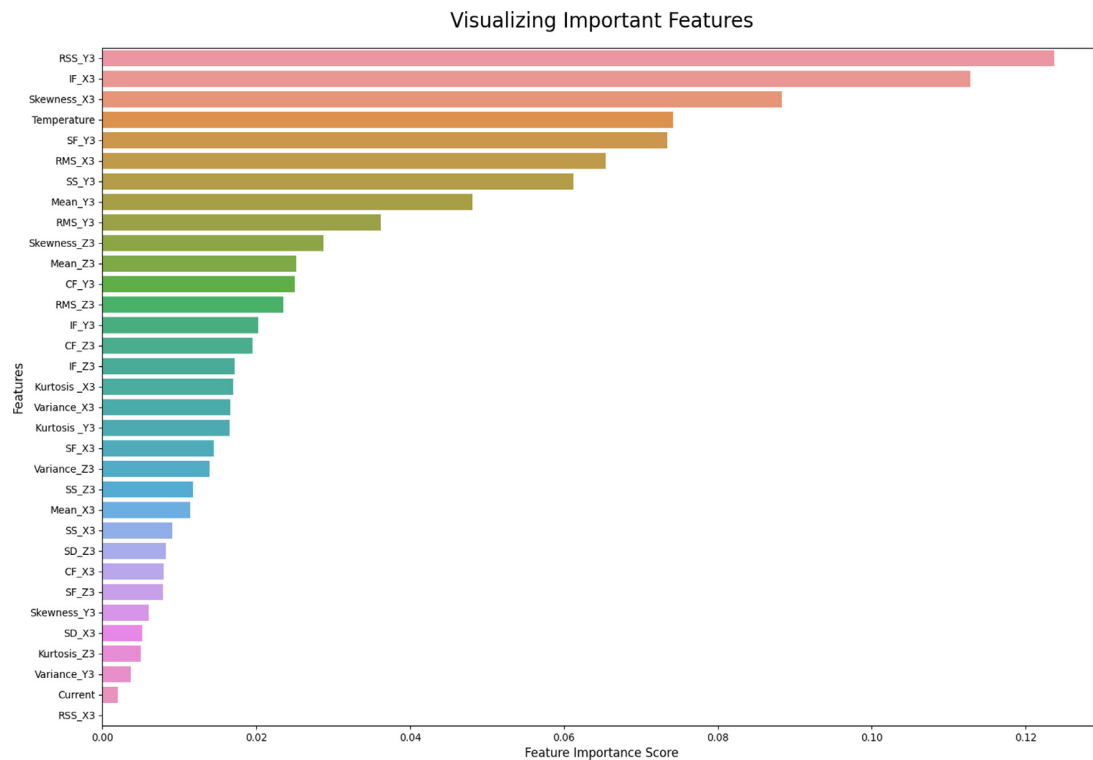
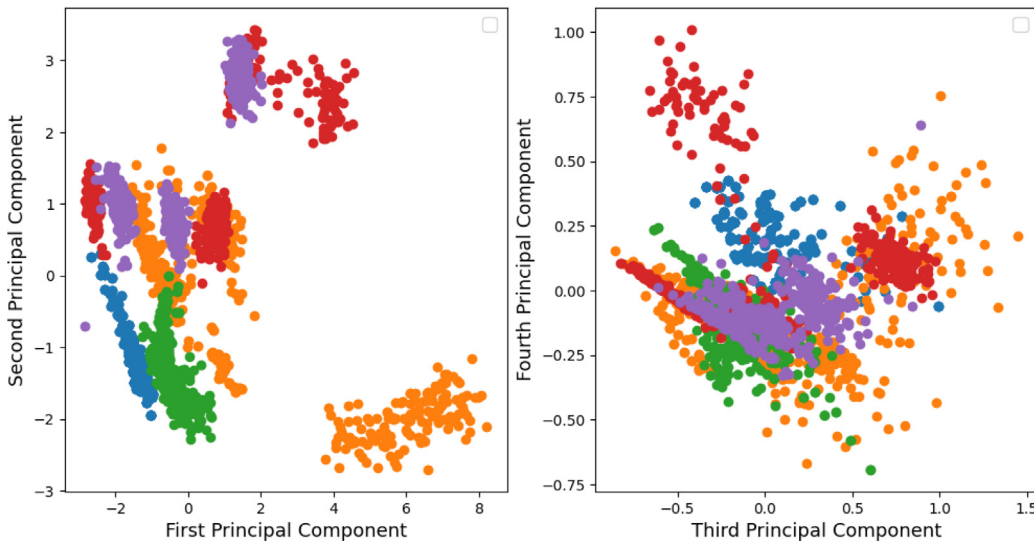
Regarding explainability, feature ranking has an advantage because it directly ranks features based on their relevance to the target variable. This can help in understanding the significance of individual features in the context of a specific task. In our case, we used the feature ranking technique for further analysis. It is also worth noting that, in some cases, a combination of these techniques may be beneficial. As shown in Fig. 7, the first and second principal components classify the data better than the third and fourth.

2.4. Multi-class classification algorithms

The challenge of categorizing samples into one of three or more classes in machine learning is known as multi-class or multinomial classification [63]. In this case, we classify data into different fault classes. The following algorithms explained were used to implement multi-class classification.

2.4.1. Support Vector Machine (SVM)

Support Vector Machines (SVM) is a supervised machine learning algorithm for classification and regression tasks. SVMs are particularly effective in solving complex problems with high-dimensional data. SVM aims to find an optimal hyperplane that separates data points belonging to different classes with the most significant possible margin. Although SVM was initially designed for binary classification, several strategies exist to extend it to handle multi-class problems. The same method is applied to multi-class classification after dividing the multi-classification problem into smaller binary classification problems. Some standard techniques for performing multi-classification using SVM are: “One versus One” (OVO), “One vs All” (OVA), and “Directed Acyclic Graph” (DAG) strategy. It is seen that OVO is the method that is superior as compared to others [64].

**Fig. 6.** Feature ranking using random forest classifier.**Fig. 7.** Principal component analysis.

2.4.2. Random Forest (RF)

An ensemble tree-based learning method is the Random Forest (RF), a supervised machine learning method used for regression and classification tasks [65]. As its name implies, the random forest algorithm builds a forest with several decision trees and averages predictions across different trees. The random forest classifier builds each tree using the bagging and random subspace methods to produce an uncorrelated forest of trees. The ultimate judgment or forecast is based on the majority of votes from each decision tree node. This learning paradigm derives its label “random” from two fundamental ideas: When creating trees, random subsets of training data are sampled, and when splitting nodes, random subsets of variables or features are considered. Random forest was also used to analyse the data.

2.4.3. Decision Tree (DT)

A Decision Tree (DT) classifier is a structured approach to multi-class classification. It asks a series of questions regarding the attributes and features of the dataset. A binary tree may be used to demonstrate the decision tree classification approach. A query is provided on the root and each internal node, and the information on that node is then separated into unique records with various features. The tree leaves indicate the several classifications that the dataset is separated into. The decision tree algorithm was also used for data analysis in this article.

2.4.4. K-nearest neighbour (KNN)

K-Nearest Neighbours (KNN) is a supervised machine learning algorithm for classification and regression tasks. KNN identifies the K-nearest neighbours in the training dataset for a given test data point.

based on the chosen distance metric. The class label of the test point is determined by majority voting among its K-nearest neighbours. The class that occurs most frequently among the K-neighbours is assigned as the predicted class label for the test point. KNN was used for data analysis.

2.4.5. Logistic Regression (LR)

Logistic Regression (LR) is a supervised machine learning algorithm used for binary classification tasks. Despite its name, logistic regression is primarily used for classification rather than regression. Logistic regression can also be extended to handle multi-class classification problems using techniques like One-vs-Rest (OvR) or softmax regression. OvR trains multiple logistic regression models, each considering one class positive and the rest negative. Softmax regression generalizes logistic regression to handle multiple classes directly, using a softmax function to compute class probabilities. A logistic regression algorithm was used in this article for data analysis.

2.4.6. Multinomial Naïve Bayes (MNB)

Multinomial Naive Bayes (MNB) is a probabilistic algorithm, especially when dealing with multiple classes. It assumes that the features follow a multinomial distribution. The algorithm will estimate the probabilities of each class based on the frequency of features in the training data. It assumes that the features are conditionally independent given the class. Multinomial Naive Bayes assumes independence between features, which may not always hold in real-world scenarios. Therefore, assessing whether this assumption aligns with your dataset and problem domain is essential.

2.5. Explainable AI (XAI)

It is essential for any Machine Learning (ML) or Deep Learning (DL) model to be transparent by explaining why a particular decision was taken. It helps the decision maker or the maintenance engineer to have more visibility and trust in the decision made by the AI model. Various AI models are classified as glass box models and black box models concerning the interpretability of the model. Interpretability is related to the ability to understand the outcome or not. Decision Tree (DT) and Logistic Regression (LR) are “by design” interpretable models. In comparison, other models are challenging to interpret by design and are called black box models. Based on this, two ways exist to create an explainable machine-learning procedure [66]. Either you use an intrinsically interpretable predictive model, for instance, using rule-based algorithms, or you use a black-box model plus a surrogate model to explain it. This article considers the example of “Random Forest”, which is an intrinsically explainable model and “Local Interpretable Model Agnostic Explanation (LIME)”, which can be used along with a black box model to interpret an outcome.

2.5.1. Random forest as XAI

A decision tree is frequently used for the feature importance of linear and non-linear models and is an explainable machine learning model all by itself. It is a rather straightforward approach, and visualizing the tree makes it easier to understand a decision. The Random Forest (RF) classifier is a popular model that overcomes the overfitting issue that the Decision Tree (DT) models frequently face. RF generates multiple decision trees, which are combined to make a more accurate prediction. The RF can be used to rank the features as we did in the earlier section to understand feature importance in decision-making. Another way to visualize is using the tree plot, which explains a particular classification made by the RF model.

2.5.2. LIME

LIME (Local Interpretable Model-agnostic Explanations) is a popular technique for interpreting machine learning models, including those trained on tabular data. LIME provides local explanations for individual predictions, helping to understand how the model arrived at its decisions. The working principle of LIME for tabular data involves the following steps:

- The first step is to pre-process the tabular data. This typically involves standardizing or normalizing numerical features, encoding categorical variables, and handling missing values.
- LIME starts by selecting an instance from the tabular dataset for which you want an explanation. LIME creates perturbed versions to understand the model’s behaviour around this instance. Perturbations involve randomly modifying or sampling from the original instance while preserving the marginal distribution of each feature.
- The perturbed instances are then passed through the trained model, and their predictions are obtained. The goal is to gather sufficient information about how the model behaves in the local neighbourhood of the selected instance.
- LIME uses the predictions from the perturbed instances to build local linear models as explanations. It assigns weights to each perturbed instance based on its proximity to the original instance. The weights can be determined using various methods, such as kernel functions or distance metrics.
- Once the local linear models are created, LIME calculates the importance of each feature for the model’s predictions. This is done by examining the coefficients or weights assigned to the features in the linear models. Higher weights indicate greater importance, while close to zero or zero weights suggest that the feature has little influence on the predictions.
- Finally, LIME generates an explanation by presenting the top features with their corresponding importance values. These explanations help in understanding the model’s decision-making process at a local level, providing insights into why a particular prediction was made.

It is important to note that LIME is model-agnostic, meaning it can be used with any black-box model, including complex models like neural networks, decision trees, or random forests. By providing local explanations, LIME helps to increase the transparency and interpretability of these models, enabling users to trust and validate their decisions.

3. Results

This section discusses the results obtained using the proposed data acquisition system using frequency domain data, as discussed in earlier sections.

3.1. Outcome

This section analyses the four cases of feature sets as discussed in Section 2.3: Single-sensor Single-location, Single-sensor Multi-location, Multi-sensor Single-location, Multi-sensor Multi-location for five class classifications (no fault, single-plane unbalance, two-plane rotor unbalance, offset misalignment and component looseness). Note that the feature sets were standardized and normalized. As discussed earlier, a high dimensional feature set was used (especially in the case of Multi-sensor Multi-location and Single-sensor Multi-location). Hence, feature selection techniques were used. Random forest classifier and XGBoost classifier techniques were used for each case. Temperature and vibration sensors have contributed to the decision-making when multiple sensors are used.

Training, testing and validation accuracy after applying SVM, Random Forest, Decision Tree, KNN, Logistic Regression and Multinomial

Table 8
Results for training accuracy.

Training accuracy																		
Sr. No.	Combination	Single-sensor Single-location Sensor: Vibration Location: 3				Single-sensor Multi-location Sensor: Vibration Location: 1, 2, 3, 4				Multi-sensor Multi-location Sensor: Vibration, Temperature, Current Location: 1, 2, 3, 4				Multi-sensor Single-location Sensor: Vibration, Temperature, Current Location: Nearest to fault				Support
		Accuracy	Precision	Recall	F1 Score	Accuracy	Precision	Recall	F1 Score	Accuracy	Precision	Recall	F1 Score	Accuracy	Precision	Recall	F1 Score	
1.	Support Vector Machine	0.79	0.83	0.79	0.80	0.64	0.74	0.64	0.61	0.82	0.82	0.81	0.95	0.95	0.95	0.95	1575	
2.	Random Forest	1.00	1.00	1.00	1.00	1.00	1.00	1.00	1.00	1.00	1.00	1.00	1.00	1.00	1.00	1.00	1575	
3.	Decision Tree	0.85	0.87	0.85	0.85	0.86	0.91	0.86	0.86	0.92	0.92	0.92	0.95	0.95	0.95	0.95	1575	
4.	K-Nearest Neighbours	0.93	0.93	0.93	0.93	0.93	0.93	0.93	0.93	0.99	0.99	0.99	0.99	0.99	0.99	0.99	1575	
5.	Logistic Regression	0.80	0.81	0.80	0.80	0.77	0.78	0.77	0.77	0.87	0.87	0.87	0.91	0.91	0.91	0.91	1575	
6.	Multinomial naive bayes	0.73	0.78	0.73	0.73	0.53	0.50	0.53	0.50	0.67	0.68	0.67	0.71	0.74	0.71	0.71	1575	

Table 9
Results for testing accuracy.

Testing accuracy																		
Sr. No.	Combination	Single-sensor Single-location Sensor: Vibration Location: 3				Single-sensor Multi-location Sensor: Vibration Location: 1, 2, 3, 4				Multi-sensor Multi-location Sensor: Vibration, Temperature, Current Location: 1, 2, 3, 4				Multi-sensor Single-location Sensor: Vibration, Temperature, Current Location: Nearest to fault				Support
		Accuracy	Precision	Recall	F1 Score	Accuracy	Precision	Recall	F1 Score	Accuracy	Precision	Recall	F1 Score	Accuracy	Precision	Recall	F1 Score	
1.	Support Vector Machine	0.76	0.80	0.76	0.76	0.64	0.75	0.64	0.62	0.79	0.79	0.79	0.78	0.95	0.95	0.95	0.95	338
2.	Random Forest	0.97	0.97	0.97	0.97	0.97	0.97	0.97	0.97	0.99	0.99	0.99	0.99	1.00	1.00	1.00	1.00	338
3.	Decision Tree	0.81	0.85	0.81	0.81	0.81	0.90	0.81	0.82	0.91	0.92	0.91	0.91	0.93	0.94	0.93	0.94	338
4.	K-Nearest Neighbours	0.85	0.86	0.85	0.85	0.83	0.84	0.83	0.84	0.99	0.99	0.99	0.99	0.99	0.99	0.99	0.99	338
5.	Logistic Regression	0.79	0.81	0.79	0.79	0.75	0.76	0.75	0.74	0.86	0.87	0.86	0.86	0.91	0.91	0.91	0.91	338
6.	Multinomial naive bayes	0.74	0.80	0.74	0.75	0.54	0.50	0.54	0.50	0.66	0.68	0.66	0.66	0.70	0.73	0.70	0.69	338

Naïve Bayes for all four cases using all features for five class classifications are shown in Table 8, Tables 9 and 10, respectively. The table compares the accuracy, precision, recall, and F1 score of all 4 cases. “Support” is a term used to describe the sample size for a specific class within the dataset.

Testing confusion matrix for Multi-sensor Single-location case using SVM, Random Forest, Decision Tree, KNN, Logistic Regression, and Multinomial Naïve Bayes are shown in Fig. 8. A confusion matrix is a fundamental tool for evaluating a classification model. It breaks down the model's predictions into four categories: True Positives (correct positive predictions), True Negatives (correct negative predictions), False Positives (incorrect positive predictions), and False Negatives (incorrect negative predictions). These elements calculate essential metrics like accuracy, precision, recall, and the F1 score, providing insights into the model's performance.

The four cases were analysed to check the performance. It was observed that Multi-sensor Single-location showed the highest performance, followed by Multi-sensor Multi-location, Single-sensor Multi-location, and Single-sensor Single-location. It can be seen that the use of multiple sensors has increased the performance of AI models. Multi-sensor Single-location case had the highest 100% testing accuracy using Random Forest, 99% using KNN, 95% using SVM, 93% using Decision Tree, 91% using Logistic Regression, and 70% using Multinomial Naïve Bayes. In this case, multiple sensors (accelerometer, temperature, and current sensor) were placed nearest the fault location. Following, better accuracy was achieved using the Multi-sensor Multi-location case. Here, the highest accuracy of 99% was obtained using Random Forest and KNN, approx. 86% using Logistic Regression, 79% using SVM and approx. 66% using Multinomial Naïve Bayes algorithm. Multiple sensors were used in the Multi-sensor Multi-location case, but the data from sensors placed at all four bearing locations were

Table 10
Results for validation accuracy.

Validation accuracy																		
Sr. No.	Combination	Single-sensor Single-location Sensor: Vibration Location: 3				Single-sensor Multi-location Sensor: Vibration Location: 1, 2, 3, 4				Multi-sensor Multi-location Sensor: Vibration, Temperature, Current Location: 1, 2, 3, 4				Multi-sensor Single-location Sensor: Vibration, Temperature, Current Location: Nearest to fault				Support
		Accuracy	Precision	Recall	F1 Score	Accuracy	Precision	Recall	F1 Score	Accuracy	Precision	Recall	F1 Score	Accuracy	Precision	Recall	F1 Score	
1.	Support Vector Machine	0.78	0.81	0.78	0.79	0.68	0.81	0.68	0.65	0.84	0.83	0.84	0.83	0.96	0.96	0.96	0.95	337
2.	Random Forest	0.98	0.98	0.98	0.98	0.97	0.97	0.97	0.97	0.99	0.99	0.99	0.99	0.99	0.99	0.99	0.99	337
3.	Decision Tree	0.82	0.84	0.82	0.82	0.83	0.90	0.83	0.84	0.91	0.92	0.91	0.91	0.94	0.94	0.94	0.94	337
4.	K-Nearest Neighbours	0.86	0.86	0.86	0.86	0.83	0.84	0.83	0.84	0.97	0.97	0.97	0.97	0.99	0.99	0.99	0.99	337
5.	Logistic Regression	0.81	0.82	0.81	0.81	0.79	0.80	0.79	0.79	0.87	0.88	0.87	0.87	0.92	0.92	0.92	0.92	337
6.	Multinomial naive bayes	0.76	0.80	0.76	0.76	0.53	0.48	0.53	0.49	0.65	0.66	0.65	0.65	0.70	0.73	0.70	0.70	337

considered for analysis. In the Single-sensor Multi-location case, single sensors were used for data collection from all four bearing locations, as in the previous case. Here, the highest accuracy of 97% was obtained using Random Forest, 83% using KNN, 81% using Decision Tree, 75% using Logistic Regression, 64% using SVM, and 54% using Naïve Bayes. The lowest accuracy was obtained using the case of a Single-sensor Single-location. Here, Random Forest gave the highest accuracy of 97%, followed by 85% using KNN, 81% using Decision Tree, 79% using Logistic Regression, 76% using SVM and 54% using Multinomial Naïve Bayes. In this case, single sensors were used, keeping the location constant (not necessarily near the fault location). Based on this observation and the feature ranks, as shown in Fig. 6, it can be concluded that multiple sensors used for analysis give better results than single sensors. Also, the data collected by the sensors nearest to the fault locations enhances the classification performance. Of all the multi-class classification algorithms used, the Random Forest algorithm has shown the highest accuracy for multi-fault diagnosis using multi-sensor data fusion.

Fig. 9 shows the learning curve plotted for the Random Forest classifier. The figure has three different plots. The learning curve is shown in the first plot. The training score remains high regardless of the size of the training set. At the same time, the test score increases with the size of the training dataset up to a point where it reaches a plateau. This implies that acquiring new data to train the model might not be useful since the model's generalization performance does not increase anymore. In addition to the learning curve, the scalability of the predictive models in terms of training times can be examined. The second plot (scalability of the model) depicts the times the models require to train with various training dataset sizes. The third plot (performance plot) shows how long it took to train the models for various training sizes. In this plot, we can look for the inflection point for which the accuracy no longer increases and only the training time increases.

3.2. Explainable AI using random forest

Fig. 10 represents the Random Forest of the Multi-sensor Single-location case. RF visualization can assist us in intuitively evaluating the model's accuracy and may even help it improve.

3.3. Explainable AI using LIME

In this section, let us analyse the outcome predicted by various AI models using LIME. Fig. 11 shows a typical outcome that the LIME explainer would give. The figure shows the explanation of the 321st instance from the test data as the Random Forest classifier predicted. It can be seen that the model has predicted the outcome as 'looseness' with 100% confidence. LIME identifies the most influential features contributing to the model's decision for the selected instance. LIME assigns weights to the selected features to quantify their importance. These weights indicate each feature's impact on the model's prediction for the instance. Higher weights indicate stronger influence, while weights close to zero or zero suggest minimal impact. In this case, the feature RMS has the highest influence in deciding the outcome. The weights can be represented using different graphical elements, such as bar lengths or colour intensity, to visually indicate their influence. Along with the weights, LIME also gives an explanation based on the value of features. The feature representation and its corresponding value may not directly correspond to the actual feature values present in the original dataset. For example, if RMS is greater than 70.22, the Mean is greater than 0.12, the table on the right represents the feature and its value, etc. These values are generated and manipulated by LIME during the perturbation process.

Fig. 12 compares the prediction probabilities for different AI models for the 321st instance from the test set. The instance depicts the fault 'looseness'. Also, all the AI models assign a higher probability to class 'looseness'. It can be seen that models such as Random Forest and KNN accurately predict the fault as 'looseness' with 100% confidence. However, the Decision Tree predict the outcome as Looseness with 78% confidence, Logistic Regression with 61% confidence, Multinomial Naïve Bayes with 87% confidence and SVM predict 'Looseness' fault with 72% confidence.

In each algorithm, the probability values for each class differ because the feature weights calculated by each algorithm are unique. By considering the feature values and their assigned weights, the algorithm determines the likelihood of each class and selects the one with the highest probability as its prediction. These outcomes can be analysed by a domain expert to identify which algorithm captures the relevant signals or features for accurate predictions. Hence, the black box algorithms have transformed into transparent white box models, enabling us to understand the factors influencing their predictions.

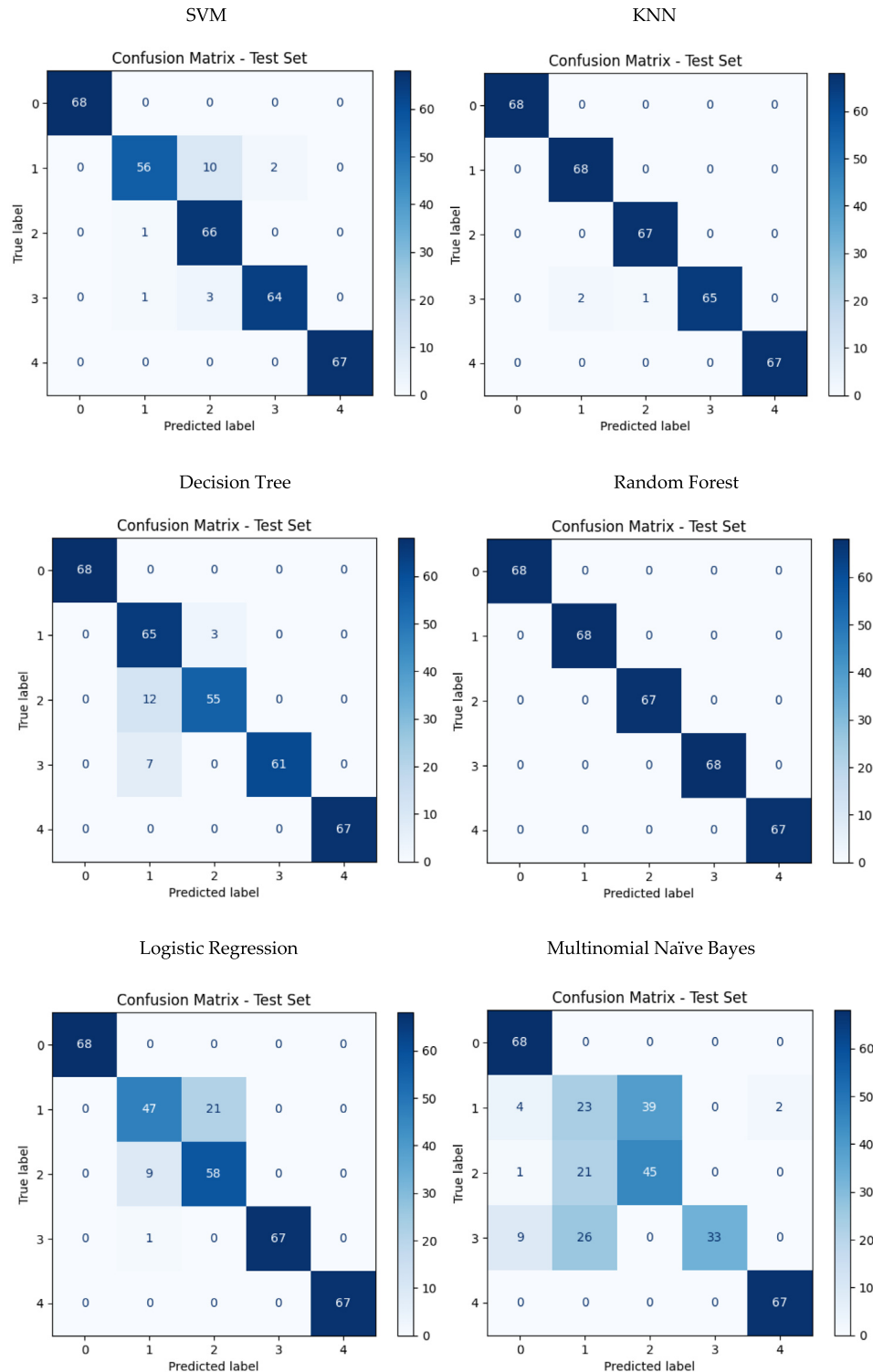


Fig. 8. Confusion matrix for multi-sensor single-location.

Fig. 13 shows the local explanation by depicting feature contribution towards each class using LIME. This approach allows you to visualize the explanations for each class separately, gaining insights into the feature importance for each class prediction in a multi-class classification scenario. Fig. 14 visualizes the actual global feature importance weights obtained from Random Forest and Decision Tree models. The importance is sorted in descending order to visualize the most important features at the top.

4. Discussion

4.1. Challenges and limitations in multi-fault diagnosis

- Data Availability: Simulating the industrial conditions in the test setup for data acquisition is challenging. Inducing one type of fault may also lead to another fault. Hence, utmost care must be taken while inducing the fault for DAQ.

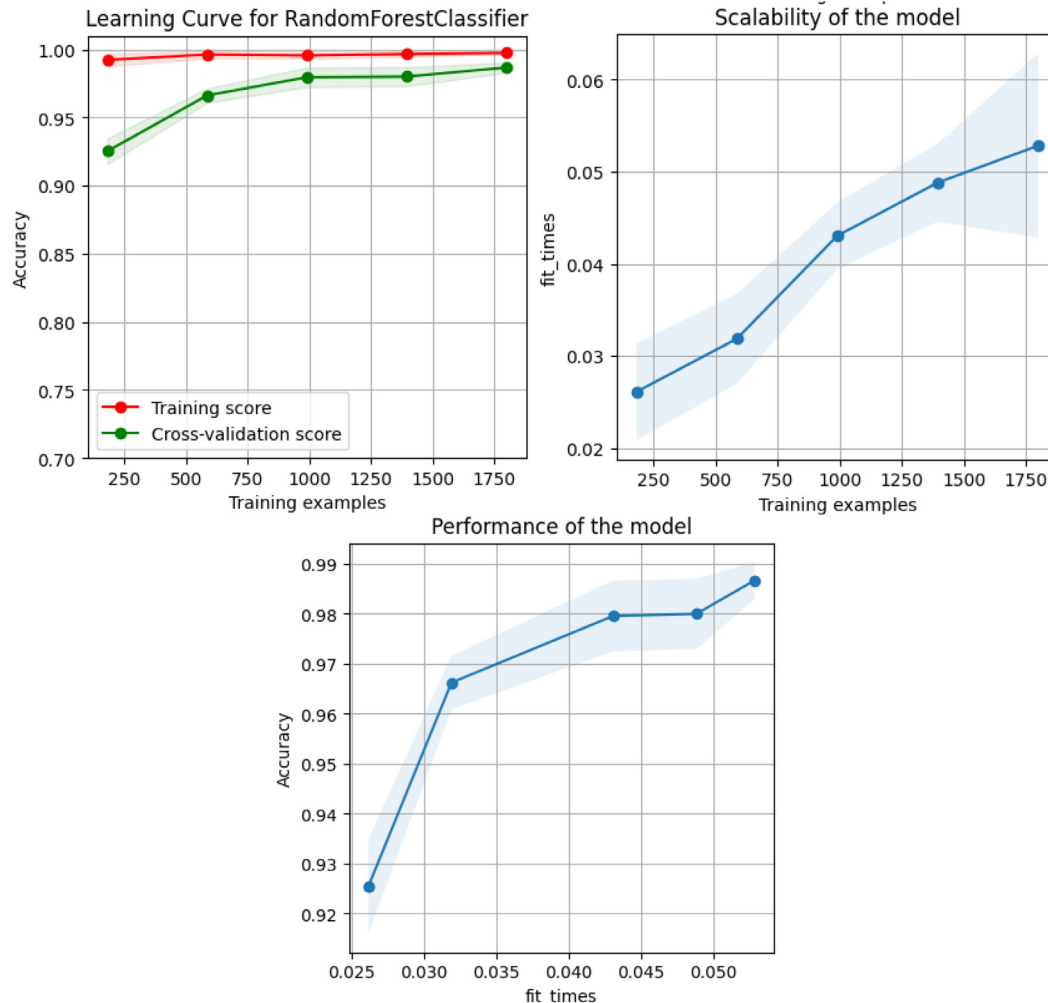


Fig. 9. The learning curve for the Random Forest classifier.

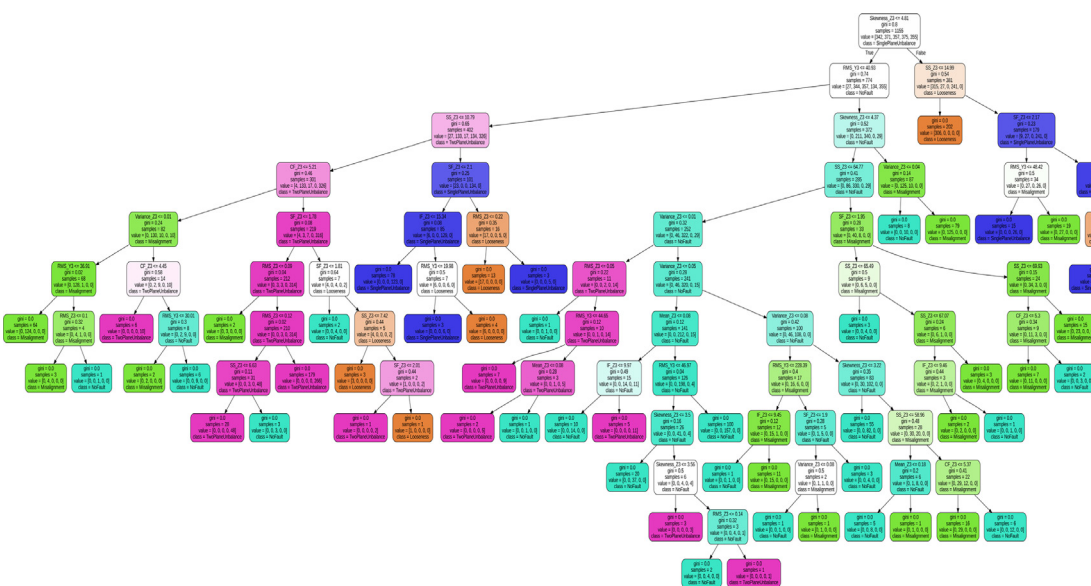


Fig. 10. Random Forest for Multi-sensor Single-location case.

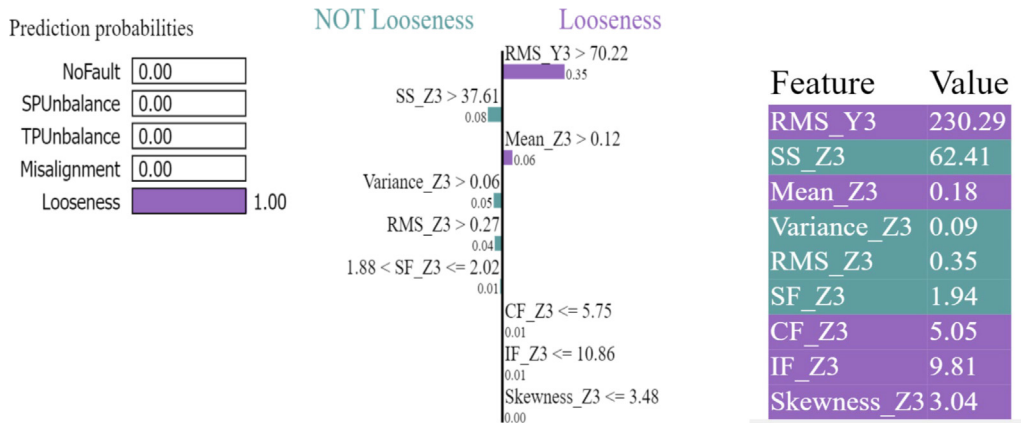


Fig. 11. Visual explanation by LIME for the outcome generated by Random Forest Classifier.

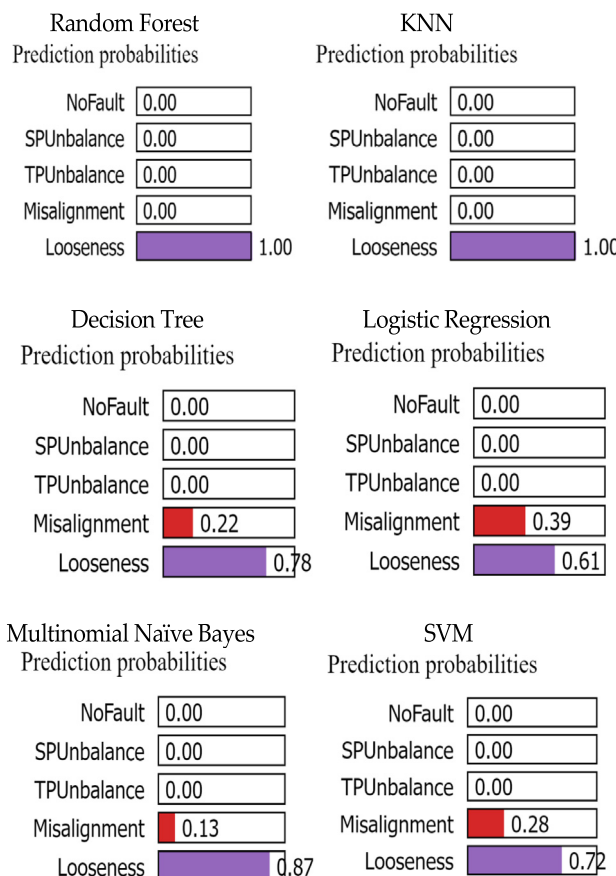


Fig. 12. Comparison of prediction probabilities for various AI models using LIME.

- Sensor fusion: It is a technique for combining data from several sensors (homogeneous or heterogeneous) into a single data point. Choosing appropriate peripherals for each sensor is essential for effective data fusion.
- Class Imbalance: It is easier to get healthy data from the machine than unhealthy data. This may lead to class Imbalance in machine learning.
- Algorithm Validation: To increase the credibility of predictive maintenance, it is again essential to simulate the AI algorithms on test setup data and implement them on real-time industrial data.

- Interpretability: Non-interpretability of AI models makes it difficult for users to understand why the model made a particular diagnosis/ classification.

4.2. Recommendations for future work

Following are some recommendations for future work in the domain:

- Current research focuses on data from test setups which cannot completely resemble the industrial environment. Collecting

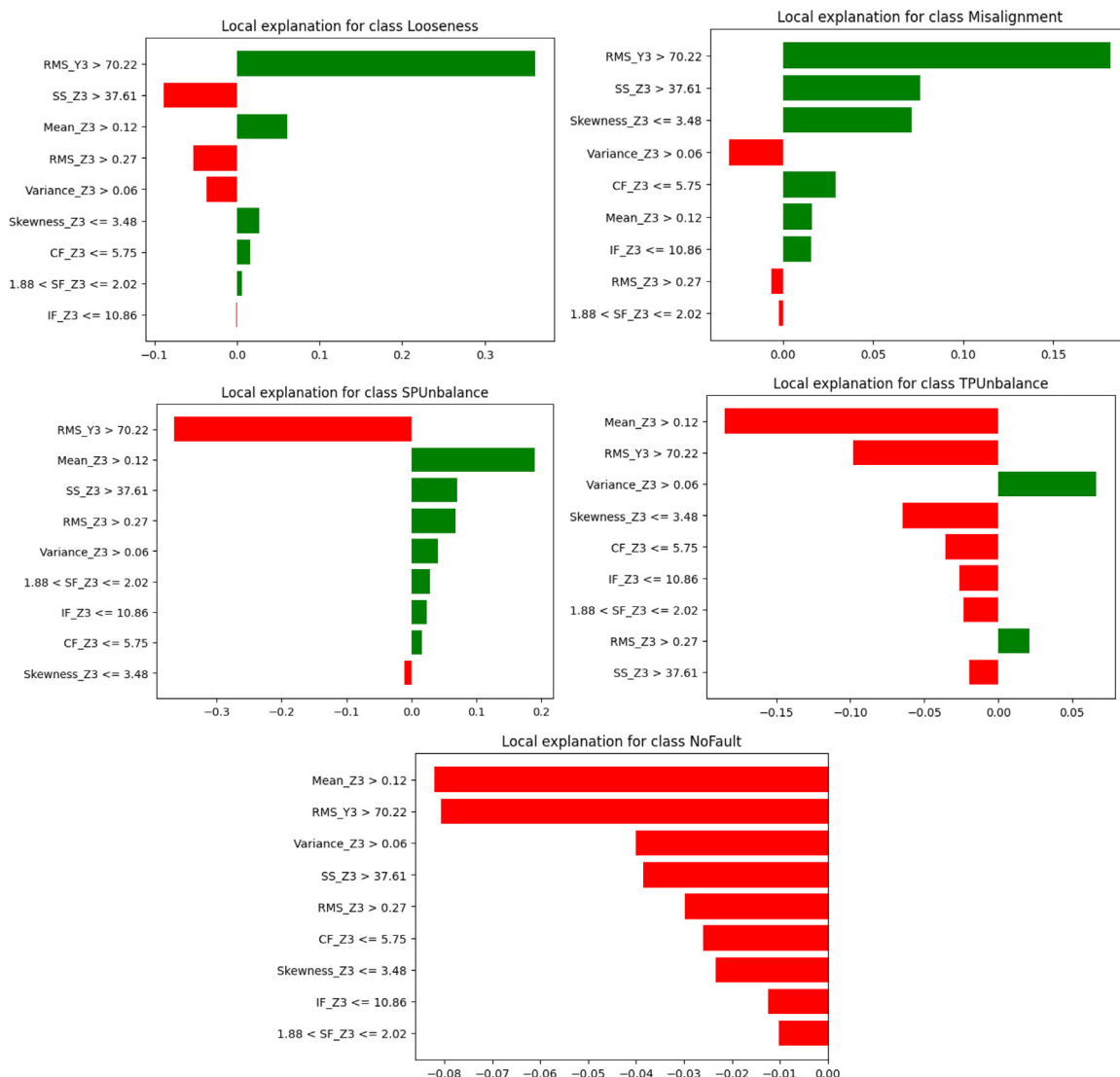


Fig. 13. Local explanations of fault classes using LIME.

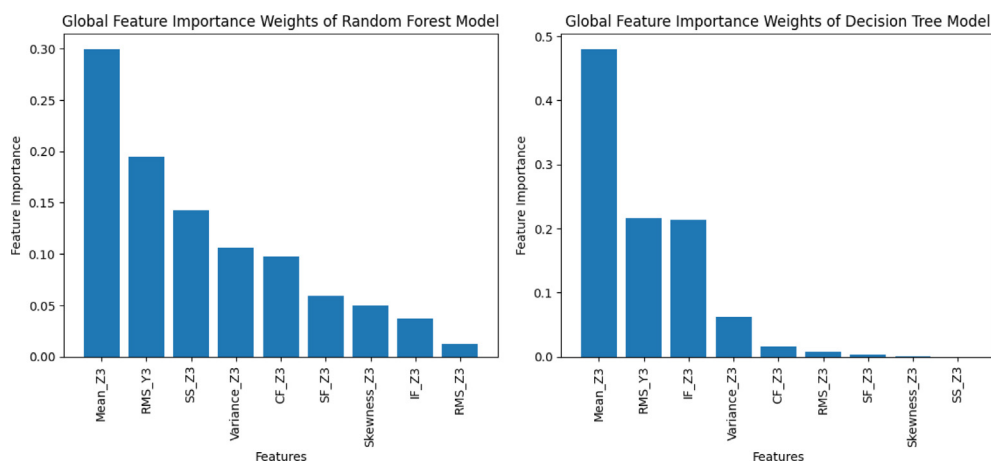


Fig. 14. Global feature importance weights of Random Forest and Decision Tree model.

the data from real-time industrial machinery can improve the diversity of conditions.

- Decisions made by most of the AI models are not interpretable, making it difficult for users to understand why a particular decision was made. Explainable AI can be a potential way to increase the interpretability of a decision made by an AI model. Counterfactual explanations are needed for providing solutions to predictive maintenance issues.
- Digital Twin technology can be associated with predictive maintenance for inaccessible or remote fault diagnosis.
- Different condition monitoring techniques are used for different types of faults. Multiple condition monitoring techniques can be fused for multiple fault diagnosis.
- Bearing defects are the subject of much research. However, industrial rotating machines have defects such as unbalance, misalignment, looseness, and so on, all related to one another. There is a need to consider the interdependence of faults while considering multiple fault diagnosis.
- AI model trained to work on one dataset gives comparatively less accuracy on a different dataset. For future research, domain adaptation in AI for multi-fault diagnosis needs to be considered.

4.3. Conclusion

The study systematically implements Explainable predictive maintenance for numerous fault diagnostics in rotating machines, including no-fault, overhung rotor unbalance, two-plane rotor unbalance, offset misalignment, component looseness, and bearing defects using AI and XAI techniques. Previous research has mainly concentrated on the fault diagnosis and prognosis. To the best of our knowledge, limited work has been done in implementing multi-sensor data fusion for multiple fault diagnosis and explaining the diagnosis predicted by AI models using XAI. The results conclude the following:

- Frequency domain analysis using FFT raw data can reveal more information based on frequency features that are difficult to detect in the time domain. The frequency domain data collected can also be validated using real-time industrial devices. Hence, using FFT raw data in data-driven predictive maintenance of rotating machines is advisable.
- The authors had done analysis using single sensors and multiple sensors (vibration, temperature, current). It was seen that the data from multiple sensors enhanced the accuracy of results. Each sensor is related to a particular condition-monitoring technique. Also, some techniques are specifically used for detecting a particular fault. Hence, using multiple sensors allows fusing multiple condition monitoring techniques for predictive maintenance, allowing scope to diagnose more faults.
- The sensor's location plays a vital role in fault diagnosis accuracy. The accuracy of results was high for sensors close to the fault location.
- Collecting data from a test setup gives more data freedom than online datasets available. The authors built the test setup, which saved the cost compared to the purchase of the test setup. It is also advisable to make the own test setup under the guidance of condition monitoring experts.
- In practical cases, it is seen that one fault gives rise to another fault. Hence, there is a possibility of multiple faults in the test setup in the real-time industrial environment and while collecting data for research purposes. It is crucial to consider the interdependence of faults in rotating machines.
- Explainable AI techniques, especially LIME, gave a deeper insight into the classification implemented by the AI model, thus increasing the trust in the outcome predicted by the AI model.

Considering the factors discussed above, multi-sensor data fusion-based multi-fault diagnosis in rotating machines gave considerable accuracy and convincing validity using the FFT raw data. Embedding a more significant number of faults and enhancing the interpretability of the classification by AI models will be the future aim of the research.

CRediT authorship contribution statement

Shreyas Gawde: Conceptualization, Data curation, Formal analysis, Methodology, Writing – original draft. **Shruti Patil:** Conceptualization, Formal analysis, Methodology, Project administration, Supervision, Validation, Visualization, Writing – review & editing. **Satish Kumar:** Conceptualization, Formal analysis, Methodology, Project administration, Supervision, Validation, Visualization, Writing – review & editing. **Pooja Kamat:** Conceptualization, Supervision, Validation, Writing – review & editing. **Ketan Kotecha:** Conceptualization, Supervision, Validation, Visualization, Writing – review & editing.

Declaration of competing interest

The authors declare that they have no known competing financial interests or personal relationships that could have appeared to influence the work reported in this paper.

Data availability

Data will be made available on request.

Acknowledgements

We acknowledge the support extended by Mr. Suryakant Gawde, M Insight Services, Goa, India, in fault simulation for data collection.

Appendix A. Supplementary data

Supplementary material related to this article can be found online at <https://doi.org/10.1016/j.dajour.2024.100425>.

References

- [1] J.S. Rapur, R. Tiwari, Automation of multi-fault diagnosing of centrifugal pumps using multi-class support vector machine with vibration and motor current signals in frequency domain, *J. Brazilian Soc. Mech. Sci. Eng.* 40 (6) (2018) <http://dx.doi.org/10.1007/s40430-018-1202-9>.
- [2] P. Ong, Y.K. Tan, K.H. Lai, C.K. Sia, A deep convolutional neural network for vibration-based health-monitoring of rotating machinery, *Decis. Anal.* 7 (2023) 100219, <http://dx.doi.org/10.1016/j.dajour.2023.100219>.
- [3] J. Sobral, A. Roque, *Predictive maintenance using ultrasound technology as condition monitoring*, 2018.
- [4] D. Lopez-Perez, J. Antonino-Daviu, Application of infrared thermography to failure detection in industrial induction motors: Case stories, *IEEE Trans. Ind. Appl.* 53 (3) (2017) 1901–1908, <http://dx.doi.org/10.1109/TIA.2017.2655008>.
- [5] Z. Zhou, D. Chen, S. (Shengquan) Xie, Springer series in advanced manufacturing, 2007, [Online]. Available: <http://www.springer.com/series/7113%0Ahttp://linkinghub.elsevier.com/retrieve/pii/B9781856174787500118>.
- [6] S. Gawde, S. Patil, S. Kumar, K. Kotecha, A Scoping Review on Multi-Fault Diagnosis of Industrial Rotating Machines using Multi-Sensor Data Fusion (0123456789), Springer Netherlands, 2022, <http://dx.doi.org/10.1007/s10462-022-10243-z>.
- [7] S. Gawde, S. Patil, S. Kumar, P. Kamat, K. Kotecha, A. Abraham, Multi-fault diagnosis of industrial rotating machines using data-driven approach: A review of two decades of research, *Eng. Appl. Artif. Intell.* 123 (9) (2023) 1–39, <http://dx.doi.org/10.1016/j.engappai.2023.106139>, 2023.
- [8] D.J. Bordoloi, R. Tiwari, Optimum multi-fault classification of gears with integration of evolutionary and SVM algorithms, *Mech. Mach. Theory* 73 (2014) 49–60, <http://dx.doi.org/10.1016/j.mechmachtheory.2013.10.006>.
- [9] C. Xi, G. Yang, L. Liu, H. Jiang, X. Chen, A refined composite multivariate multiscale fluctuation dispersion entropy and its application to multivariate signal of rotating machinery, *Entropy* 23 (1) (2021) 1–18, <http://dx.doi.org/10.3390/e23010128>.

- [10] R.V. Sánchez, P. Lucero, R.E. Vásquez, M. Cerrada, J.C. Macancela, D. Cabrera, Feature ranking for multi-fault diagnosis of rotating machinery by using random forest and KNN, *J. Intell. Fuzzy Systems* 34 (6) (2018) 3463–3473, <http://dx.doi.org/10.3233/JIFS-169526>.
- [11] M.Z. Ali, M.N.S.K. Shabbir, S.M.K. Zaman, X. Liang, Single- and multi-fault diagnosis using machine learning for variable frequency drive-fed induction motors, *IEEE Trans. Ind. Appl.* 56 (3) (2020) 2324–2337, <http://dx.doi.org/10.1109/TIA.2020.2974151>.
- [12] D. Pagano, A predictive maintenance model using long short-term memory neural networks and Bayesian inference, *Decis. Anal.* 6 (2023) 100174, <http://dx.doi.org/10.1016/j.dajour.2023.100174>.
- [13] H. Wu, A. Huang, J. Sutherland, Layer-wise relevance propagation for interpreting LSTM-RNN decisions in predictive maintenance, *Int. J. Adv. Manuf. Technol.* 118 (2022) 1–16, <http://dx.doi.org/10.1007/s00170-021-07911-9>.
- [14] Y. Xue, D. Dou, J. Yang, Multi-fault diagnosis of rotating machinery based on deep convolution neural network and support vector machine, *Meas. J. Int. Meas. Confed.* 156 (2020) 107571, <http://dx.doi.org/10.1016/j.measurement.2020.107571>.
- [15] R. Tiwari, V. Analysis, Effect of frequency resolution on intelligent multiple fault diagnosis of induction motor based on support vector machine, 2021, no. December.
- [16] C.R. Soto-Ocampo, J.M. Mera, J.D. Cano-Moreno, J.L. Garcia-Bernardo, Low-cost, high-frequency, data acquisition system for condition monitoring of rotating machinery through vibration analysis-case study, *Sensors (Switzerland)* 20 (12) (2020) 1–19, <http://dx.doi.org/10.3390/s20123493>.
- [17] Y. Fu, Z. Gao, Y. Liu, A. Zhang, X. Yin, Actuator and sensor fault classification for wind turbine systems based on fast Fourier transform and uncorrelated multi-linear principal component analysis techniques, *Proceses* 8 (9) (2020) <http://dx.doi.org/10.3390/pr8091066>.
- [18] A. Yunusa-kaltungo, J.K. Sinha, Effective vibration-based condition monitoring (eVCM) of rotating machines, *J. Qual. Maint. Eng.* 23 (3) (2017) 279–296, <http://dx.doi.org/10.1108/JQME-08-2016-0036>, Jan.
- [19] H. Wei, Q. Zhang, M. Shang, Y. Gu, Extreme learning machine-based classifier for fault diagnosis of rotating machinery using a residual network and continuous wavelet transform, *Measurement* 183 (2021) 109864, <http://dx.doi.org/10.1016/j.measurement.2021.109864>.
- [20] R.F. Ribeiro Junior, F.A. de Almeida, G.F. Gomes, Fault classification in three-phase motors based on vibration signal analysis and artificial neural networks, *Neural Comput. Appl.* 32 (18) (2020) 15171–15189, <http://dx.doi.org/10.1007/s00521-020-04868-w>.
- [21] M.N. Utah, J.C. Jung, Fault state detection and remaining useful life prediction in AC powered solenoid operated valves based on traditional machine learning and deep neural networks, *Nucl. Eng. Technol.* 52 (9) (2020) 1998–2008, <http://dx.doi.org/10.1016/j.net.2020.02.001>.
- [22] E. Wescoat, L. Mears, J. Goodnough, J. Sims, Frequency energy analysis in detecting rolling bearing faults, *Procedia Manuf.* 48 (2020) 980–991, <http://dx.doi.org/10.1016/j.promfg.2020.05.137>.
- [23] T. Yassine, L. Sidahmed, O.Z. Mohamed, Bearing fault classification based on envelope analysis and artificial neural network, in: 2019 International Conference on Advanced Electrical Engineering, ICAEE, 2019, pp. 1–5, <http://dx.doi.org/10.1109/ICAEE47123.2019.9015123>.
- [24] X. Yan, M. Jia, A novel optimized SVM classification algorithm with multi-domain feature and its application to fault diagnosis of rolling bearing, *Neurocomputing* 313 (2018) 47–64, <http://dx.doi.org/10.1016/j.neucom.2018.05.002>.
- [25] M. Azamfar, J. Singh, I. Bravo-Imaz, J. Lee, Multisensor data fusion for gearbox fault diagnosis using 2-D convolutional neural network and motor current signature analysis, *Mech. Syst. Signal Process.* 144 (2020) 106861, <http://dx.doi.org/10.1016/j.ymssp.2020.106861>.
- [26] Y. Zhang, K. Xing, R. Bai, D. Sun, Z. Meng, An enhanced convolutional neural network for bearing fault diagnosis based on time-frequency image, *Measurement* 157 (2020) 107667, <http://dx.doi.org/10.1016/j.measurement.2020.107667>.
- [27] X. Zhou, S. Mao, M. Li, A novel anti-noise fault diagnosis approach for rolling bearings based on convolutional neural network fusing frequency domain feature matching algorithm, *Sensors* 21 (16) (2021) <http://dx.doi.org/10.3390/s21165532>.
- [28] D.J. Bordoloi, R. Tiwari, Optimum multi-fault classification of gears with integration of evolutionary and SVM algorithms, *Mech. Mach. Theory* 73 (2014) 49–60, <http://dx.doi.org/10.1016/j.mechmachtheory.2013.10.006>.
- [29] J.S. Rapur, R. Tiwari, An intelligent and robust fault diagnosis system for identification of centrifugal pump defects in frequency domain using corrupted vibration and current signatures, in: *Advances in Rotor Dynamics, Control, and Structural Health Monitoring*, 2020, pp. 407–426.
- [30] Y. Selvaraj, C. Selvaraj, Proactive maintenance of small wind turbines using IoT and machine learning models, *Int. J. Green Energy* (2021) 1–12, <http://dx.doi.org/10.1080/15435075.2021.1930004>.
- [31] L.M.F.J. Suárez, J.C.G.D.F. García, Low - cost industrial IoT system for wireless monitoring of electric motors condition, *Mob. Netw. Appl.* 28 (1) (2023) 97–106, <http://dx.doi.org/10.1007/s11036-022-02017-2>.
- [32] M. Huang, Z. Liu, Y. Tao, Simulation modelling practice and theory mechanical fault diagnosis and prediction in IoT based on multi- source sensing data fusion, *Simul. Model. Pract. Theory* (August) (2019) 101981, <http://dx.doi.org/10.1016/j.simpat.2019.101981>.
- [33] T. Mian, A. Choudhary, S. Fatima, B.K. Panigrahi, Artificial intelligence of things based approach for anomaly detection in rotating machines *, *Comput. Electr. Eng.* 109 (PA) (2023) 108760, <http://dx.doi.org/10.1016/j.compeleceng.2023.108760>.
- [34] H.Y. Chen, C.H. Lee, Vibration signals analysis by explainable artificial intelligence (XAI) approach: Application on bearing faults diagnosis, *IEEE Access* 8 (2020) 134246–134256, <http://dx.doi.org/10.1109/ACCESS.2020.3006491>.
- [35] M.J. Hasan, M. Sohaib, J.M. Kim, An explainable ai-based fault diagnosis model for bearings, *Sensors* 21 (12) (2021) <http://dx.doi.org/10.3390/s21124070>.
- [36] L.C. Brito, G. Antonio, J.N. Brito, M.A.V. Duarte, An explainable artificial intelligence approach for unsupervised fault detection and diagnosis in rotating machinery, *Mech. Syst. Signal Process.* 163 (2021) 108105, <http://dx.doi.org/10.1016/j.ymssp.2021.108105>.
- [37] N. Tritschler, A. Dugenske, T. Kurkess, An automated edge computing-based condition health monitoring system: With an application on rolling element bearings, *J. Manuf. Sci. Eng.* 143 (2021) 1–10, <http://dx.doi.org/10.1115/1.4049845>.
- [38] D.C. Sanakkayala, et al., Explainable AI for bearing fault prognosis using deep learning techniques, *Micromachines* 13 (9) (2022) <http://dx.doi.org/10.3390/mi13091471>.
- [39] V.V. Khanna, K. Chadaga, N. Sampathila, S. Prabhu, R.C.P., A machine learning and explainable artificial intelligence triage-prediction system for COVID-19, *Decis. Anal.* 7 (2023) 100246, <http://dx.doi.org/10.1016/j.dajour.2023.100246>.
- [40] Y.-C. Wang, T. Chen, M.-C. Chiu, An explainable deep-learning approach for job cycle time prediction, *Decis. Anal.* 6 (2023) 100153, <http://dx.doi.org/10.1016/j.dajour.2022.100153>.
- [41] S.J. Upasane, H. Hagras, M.H. Anisi, S. Savill, I. Taylor, K. Manousakis, A type-2 fuzzy based explainable AI system for predictive maintenance within the water pumping industry, *IEEE Trans. Artif. Intell.* (2023) 1–14, <http://dx.doi.org/10.1109/TAI.2023.3279808>.
- [42] S. Kawakura, M. Hirafuji, S. Ninomiya, R. Shibasaki, Analyses of diverse agricultural worker data with explainable artificial intelligence: XAI based on SHAP, LIME, and LightGBM, *Eur. J. Agric. Food Sci.* 4 (6) (2022) 11–19, <http://dx.doi.org/10.24018/ejfood.2022.4.6.348>.
- [43] O.A. Wahab, Explainable trust-aware selection of autonomous vehicles using LIME for one-shot federated learning, 2023, <http://dx.doi.org/10.1109/IWCMC58020.2023.10182876>, no. May.
- [44] V. Wagle, K. Kaur, P. Kamat, S. Patil, K. Kotcha, Explainable AI for multimodal credibility analysis: Case study of online beauty health(Mis)-Information, *IEEE Access PP* (2021) <http://dx.doi.org/10.1109/ACCESS.2021.3111527>.
- [45] G. Agarwal, et al., Explainable AI for ML jet taggers using expert variables and layerwise relevance propagation, *J. High Energy Phys.* 2021 (5) (2021) [http://dx.doi.org/10.1007/JHEP05\(2021\)208](http://dx.doi.org/10.1007/JHEP05(2021)208).
- [46] N. Herwig, Z. Peng, P. Borghesani, Bridging the trust gap: Evaluating feature relevance in neural network-based gear wear mechanism analysis with explainable AI, *Tribol. Int.* 187 (2023) 108670, <http://dx.doi.org/10.1016/j.triboint.2023.108670>.
- [47] P. Chandre, et al., Explainable AI for intrusion prevention: A review of techniques and applications, 2023, pp. 339–350, http://dx.doi.org/10.1007/978-99-3758-5_31.
- [48] M. Jahangoshai, M. Abbaspour, M. Saberi, Engineering applications of artificial intelligence a data-driven decision support framework for DEA target setting : an explainable AI approach, *Eng. Appl. Artif. Intell.* 127 (PA) (2024) 107222, <http://dx.doi.org/10.1016/j.engappai.2023.107222>.
- [49] W. Mao, W. Feng, Y. Liu, D. Zhang, X. Liang, A new deep auto-encoder method with fusing discriminant information for bearing fault diagnosis, *Mech. Syst. Signal Process.* 150 (2021) 107233, <http://dx.doi.org/10.1016/j.ymssp.2020.107233>.
- [50] Y. Zhou, A. Kumar, C. Parkash, G. Vashishtha, H. Tang, J. Xiang, A novel entropy-based sparsity measure for prognosis of bearing defects and development of a sparsogram to select sensitive filtering band of an axial piston pump, *Measurement* 203 (2022) 111997, <http://dx.doi.org/10.1016/j.measurement.2022.111997>.
- [51] S. Sayyad, V.C. S. Kumar, A. Bongale, K. Kotcha, A. Abraham, Remaining useful-life prediction of the milling cutting tool using time-frequency-based features and deep learning models, 23, 2023, p. 5659, <http://dx.doi.org/10.3390/s23125659>.
- [52] S.S. Udmale, S.K. Singh, Application of spectral kurtosis and improved extreme learning machine for bearing fault classification, *IEEE Trans. Instrum. Meas.* 68 (11) (2019) 4222–4233, <http://dx.doi.org/10.1109/TIM.2018.2890329>.
- [53] N. Sepulveda, J. Sinha, Theoretical validation of earlier developed experimental rotor faults diagnosis model, *Int. J. Hydromechatronics* 4 (2021) 295, <http://dx.doi.org/10.1504/IJHM.2021.118009>.
- [54] D. Zhao, W. Cheng, R.X. Gao, R. Yan, P. Wang, Generalized vold-Kalman filtering for nonstationary compound faults feature extraction of bearing and gear, *IEEE Trans. Instrum. Meas.* 69 (2) (2020) 401–410, <http://dx.doi.org/10.1109/TIM.2019.2903700>.

- [55] K.-B. Lee, H.-U. Shin, Y. Bak, Chapter 11 - basic control of AC motor drives, in: F. Blaabjerg (Ed.), Control of Power Electronic Converters and Systems, Academic Press, 2018, pp. 301–329, <http://dx.doi.org/10.1016/B978-0-12-805245-7.00011-1>.
- [56] Y. Tong, J. Bai, X. Chen, Research on multi-sensor data fusion technology, *J. Phys. Conf. Ser.* 1624 (3) (2020) <http://dx.doi.org/10.1088/1742-6596/1624/3/032046>.
- [57] M. Huang, Z. Liu, Research on mechanical fault prediction method based on multifeature fusion of vibration sensing data, *Sensors (Switzerland)* 20 (1) (2020) <http://dx.doi.org/10.3390/s20010006>.
- [58] X. Niu, L. Zhu, H. Ding, New statistical moments for the detection of defects in rolling element bearings, *Int. J. Adv. Manuf. Technol.* 26 (11–12) (2005) 1268–1274, <http://dx.doi.org/10.1007/s00170-004-2109-4>.
- [59] M. Cocconcelli, G. Curcurú, R. Rubini, Statistical evidence of central moment as fault indicators in ball bearing diagnostics, *Int. Conf. Surveill.* 9; M. Cocconcelli, G. Curcurú, R. Rubini, Stat. evid. cent. moment as fault indic. ball bear. diagnostics, *Int. Conf. Surveill.* 9 (1–10) (2017) 1–10, (2017).
- [60] S. Kumar, et al., A low-cost multi-sensor data acquisition system for fault detection in fused deposition modelling, *Sensors* 22 (2) (2022) <http://dx.doi.org/10.3390/s22020517>.
- [61] S. Sayyad, V.C. S. Kumar, A. Bongale, K. Kotecha, G. Selvachandran, P. Suganthan, Tool wear prediction using long short-term memory variants and hybrid feature selection techniques, *Int. J. Adv. Manuf. Technol.* 121 (2022) 1–23, <http://dx.doi.org/10.1007/s00170-022-09784-y>.
- [62] H. Wang, G. Ni, J. Chen, J. Qu, Research on rolling bearing state health monitoring and life prediction based on PCA and internet of things with multi-sensor, *Meas. J. Int. Meas. Confed.* 157 (2020) 107657, <http://dx.doi.org/10.1016/j.measurement.2020.107657>.
- [63] M. Zhang, Z. Cai, W. Cheng, Multiple-fault diagnosis method based on multiscale feature extraction and MSVM-PPA, *Shock Vib.* 2018 (2018) <http://dx.doi.org/10.1155/2018/6209371>.
- [64] C.-W. Hsu, C.-J. Lin, A comparison of methods for multiclass support vector machines, *IEEE Trans. Neural Netw.* 13 (2) (2002) 415–425, <http://dx.doi.org/10.1109/72.991427>.
- [65] M. Nacchia, F. Fruggiero, A. Lambiase, K. Bruton, A systematic mapping of the advancing use of machine learning techniques for predictive maintenance in the manufacturing sector, *Appl. Sci.* 11 (6) (2021) 1–34, <http://dx.doi.org/10.3390/app11062546>.
- [66] D.V. Carvalho, E.M. Pereira, J.S. Cardoso, Machine learning interpretability: A survey on methods and metrics, *Electron.* 8 (8) (2019) 1–34, <http://dx.doi.org/10.3390/electronics8080832>.